Molecular Pharmacology Fast Forward. Published on December 23, 2015 as DOI: 10.1124/mol.115.101980
This article has not been copyedited and formatted. The final version may differ from this version.

Biased type 1 cannabinoid receptor signalling influences neuronal viability in a cell culture model of Huntington disease

Robert B Laprairie, Amina M Bagher, Melanie E M Kelly, Eileen M Denovan-Wright

Departments of Pharmacology and Opthamology and Visual Sciences, Dalhousie University, Halifax NS Canada B3H 4R2

Primary laboratory of origin: EMDW

Molecular Pharmacology Fast Forward. Published on December 23, 2015 as DOI: 10.1124/mol.115.101980
This article has not been copyedited and formatted. The final version may differ from this version.

Running title: Biased CB1 signalling in Huntington disease

Address for Correspondence: Eileen M Denovan-Wright, Department of Pharmacology, Dalhousie University, 5850 College St. Halifax NS CAN B3H4R2, E-mail: emdenova@dal.ca, Phone: 1.902.494.1363, Fax: 1.902.494.1388

Number of text pages: 20

Number of tables: 2

Number of figures: 5

Number of references: 61

Number of words in Abstract: 247

Number of words in Introduction: 684

Number of words in Discussion: 972

Abbreviations: 2-AG, 2-arachidonoylglycerol; AEA, anandamide; ANOVA, analysis of variance; BRET, bioluminescence resonance energy transfer; Cal-AM, calcein-AM; CB_1, type 1 cannabinoid receptor; CB_2, type 2 cannabinoid receptor; CP; CP55,940 CTx, *Cholera* toxin; CRC, concentration-response curve; EthD-1, ethidium homodimer-1; GABA, γ-aminobutyric acid; GFP^2, green fluorescent protein 2; HD, Huntington disease; mHtt, mutant huntingtin protein; PTx, *Pertussis* toxin; Rluc, *Renilla* luciferase; SEM, standard error of the mean; THC, Δ^9-tetrahydrocannabinol; WIN, WIN55,212-2;

Molecular Pharmacology Fast Forward. Published on December 23, 2015 as DOI: 10.1124/mol.115.101980
This article has not been copyedited and formatted. The final version may differ from this version.

Abstract

Huntington disease (HD) is an inherited, autosomal dominant, neurodegenerative disorder with limited treatment options. Prior to motor symptom onset or neuronal cell loss in HD, levels of the type 1 cannabinoid receptor (CB_1) decrease in the basal ganglia. Decreasing CB_1 levels are strongly correlated with chorea and cognitive deficit. CB_1 agonists are functionally selective (biased) for divergent signalling pathways. In this study, six cannabinoids were tested for signalling bias in *in vitro* models of medium spiny projection neurons expressing wild-type (ST*Hdh*$^{Q7/Q7}$) or mutant huntingtin protein (ST*Hdh*$^{Q111/Q111}$). Signalling bias was assessed using the Black and Leff operational model. Relative activity [$\Delta\log R$ (τ/K_A)] and system bias ($\Delta\Delta\log R$) were calculated relative to the reference compound WIN55,212-2 for $G\alpha_{i/o}$, $G\alpha_s$, $G\alpha_q$, $G\beta\gamma$, and β-arrestin1 signalling following treatment with 2-arachidonoylglycerol (2-AG), anandamide (AEA), CP55,940, Δ^9-tetrahydrocannabinol (THC), cannabidiol (CBD), and THC+CBD (1:1) and compared between wild-type and HD cells. The E_{max} of $G\alpha_{i/o}$-dependent ERK signalling was 50% lower in HD cells compared to wild-type cells. 2-AG and AEA displayed $G\alpha_{i/o}$/$G\beta\gamma$ bias and normalized CB_1 protein levels and improved cell viability, whereas CP55,940 and THC displayed β-arrestin1 bias and reduced CB_1 protein levels and cell viability, in HD cells. CBD was not a CB_1 agonist, but inhibited THC-dependent signalling (THC+CBD). Therefore, enhancing $G\alpha_{i/o}$-biased endocannabinoid signalling may be therapeutically beneficial in HD. In contrast, cannabinoids that are β-arrestin-biased – such as THC found at high levels in modern varieties of marijuana – may be detrimental to CB_1 signalling, particularly in HD where CB_1 levels are already reduced.

Molecular Pharmacology Fast Forward. Published on December 23, 2015 as DOI: 10.1124/mol.115.101980
This article has not been copyedited and formatted. The final version may differ from this version.

Introduction

Huntington disease

Expression of mutant huntingtin protein (mHtt) causes a myriad of molecular and cellular changes that ultimately cause progressive worsening of the symptoms of Huntington disease (HD). Early in HD progression, levels of type 1 cannabinoid receptor (CB_1) mRNA and protein decrease in medium spiny projection neurons of the caudate and putamen (Denovan-Wright and Robertson, 2000; Glass *et al.*, 2000; Van Laere *et al*., 2010). CB_1 transcription is inhibited by mHtt (McCaw *et al*., 2004; Laprairie *et al*., 2013). The reduction in CB_1 and loss of CB_1 function have been shown to contribute to the cognitive, behavioural, and motor deficits of HD pathology in animal models of HD (Blázquez *et al*., 2011; 2015; Chiarlone *et al*., 2014). Furthermore, rescue of CB_1 gene expression in the striatum using viral transduction prevents the loss of excitatory synaptic markers and reduces dendritic spine loss in animal models of HD (Naydenov *et al*., 2014). The benefit of adeno-associated viral CB_1 delivery in HD provides strong proof for the concept of treating HD through enhancing CB_1 function. However, gene-based therapies specifically for CB_1 or other single alterations in gene expression, are unlikely to be used clinically for HD in the near future because of the invasive nature of delivery and because the potential adverse effects of gene therapy are still being investigated. The more-effective gene-based therapies for HD will target the underlying cause of the disease: the *mHtt* gene and encoded protein, and not secondarily lost cellular components (Kumar *et al.,* 2015). In contrast, pharmacological strategies aimed at elevating CB_1 levels and/or signalling through remaining pool of CB_1 receptors has significant therapeutic potential for the treatment and management of HD.

Molecular Pharmacology Fast Forward. Published on December 23, 2015 as DOI: 10.1124/mol.115.101980
This article has not been copyedited and formatted. The final version may differ from this version.

Pharmacological targeting of CB_1

CB_1 is activated by cannabinoids, which are a structurally diverse group of ligands that includes endogenously occurring cannabinoids (endocannabinoids) such as anandamide (AEA) and 2-arachidonoylglycerol (2-AG), phytocannabinoids from *Cannabis sativa* such as Δ^9-tetrahydrocannabinol (THC) and synthetic cannabinoids such as CP55,940 (CP) and WIN55,212-2 (WIN) (Pertwee, 2008). Activation of CB_1 in the brain results in inhibition of neurotransmitter release from presynaptic glutamatergic and GABAergic neurons and activation of pro-survival signalling cascades such as ERK and Akt (Fernández-Ruiz, 2009). We have reported that AEA, and structurally-related compounds, increase the expression of CB_1 *via* CB_1 through $G\alpha_{i/o}$ and $G\beta\gamma$ signalling in a cell culture model expressing normal *huntingtin* (ST*Hdh*$^{Q7/Q7}$) and cells expressing mHtt (ST*Hdh*$^{Q111/Q111}$) (Laprairie *et al*., 2013). Importantly, this cell culture model endogenously expresses CB_1 and other components of the endocannabinoid system. Increasing levels of CB_1 improved neuronal viability in this cell culture model (Laprairie *et al*., 2013), lending further support to the strategy of enhancing signalling through the pool of CB_1 that are retained in the presence of mHtt and elevating CB_1 levels in these cells despite transcriptional repression *via* mHtt.

Not all cannabinoids increase CB_1 levels. THC and CP treatment promote β-arrestin-dependent CB_1 internalization and reduce CB_1-dependent downstream signalling (Laprairie *et al*., 2014). Functional selectivity (*i.e.* signalling bias) describes the receptor- and ligand-dependent enhancement of certain signal transduction pathways and the simultaneous diminution of other signal transduction pathways at a single receptor (Luttrell *et al*., 2015). Functional selectivity occurs *via* a GPCR ligand that preferentially

Molecular Pharmacology Fast Forward. Published on December 23, 2015 as DOI: 10.1124/mol.115.101980
This article has not been copyedited and formatted. The final version may differ from this version.

activates one effector (*e.g.* $G\alpha_{i/o}$) more potently and efficaciously than another (*e.g.* β-arrestin) through ligand-specific changes in GPCR conformation or dimerization with other GPCRs (Christopoulos, 2014). Signalling bias could be exploited for enhancement of CB_1 function in HD while limiting detrimental adverse on-target effects (Laprairie *et al*., 2014). Cannabinoids display signalling bias (Laprairie *et al*., 2014; Khajehali *et al.*, 2015). Endocannabinoids acting at CB_1 are $G\alpha_{i/o}$-biased whereas THC and CP are β-arrestin-biased in ST*Hdh*$^{Q7/Q7}$ cells (Laprairie *et al*., 2014). In this study, we wanted to determine how the bias of different classes of cannabinoid affected neuronal viability. We hypothesized that $G\alpha_{i/o}$-biased cannabinoids improve neuronal viability, whereas β-arrestin-biased cannabinoids reduce – or have no effect on – cell viability. The functional selectivity of 6 cannabinoids [AEA, 2-AG, THC, cannabidiol (CBD), WIN, and CP] between $G\alpha_{i/o}$-, $G\alpha_s$, $G\alpha_q$, Gβγ, β-arrestin pathways was examined in ST*Hdh*$^{Q7/Q7}$ and ST*Hdh*$^{Q111/Q111}$ cells and compared to cannabinoid-dependent changes in ATP level, GABA release, metabolic activity and cell death.

Materials and Methods

Drugs

Drugs were dissolved in ethanol (THC) or DMSO [2-AG, 8-OH-DPAT ($5HT_{1A}$ agonist), AEA, CP, CBD, gallein (Gβγ inhibitor), haloperidol (D_2 antagonist), O-2050 (CB_1 antagonist), quinpirole (D_2 agonist), WAY 100635 ($5HT_{1A}$ antagonist), WIN] and diluted to final solvent concentrations of 0.1%. 2-AG, AEA, CP, CBD, O-2050, and WIN were purchased from Tocris Bioscience (Bristol, UK). 8-OH-DPAT, haloperidol, quinpirole, THC, and WAY 100635 were purchased from Sigma-Aldrich (Oakville, ON,

Molecular Pharmacology Fast Forward. Published on December 23, 2015 as DOI: 10.1124/mol.115.101980
This article has not been copyedited and formatted. The final version may differ from this version.

CAN). The Gβγ modulator gallein was purchased from EMD Millipore (Billerica, MA). *Pertussis* toxin (PTx) and *Cholera* toxin (CTx) (Sigma-Aldrich) were dissolved in dH_2O (50 ng/mL) and added directly to the media 24 h prior to cannabinoid treatment. Pre-treatment of cells with PTx and CTx inhibits $G\alpha_{i/o}$ and $G\alpha_s$, respectively (Milligan *et al.*, 1989). In the case of CTx, this occurs *via* downregulation of $G\alpha_s$ following ADP-ribosylation (Milligan *et al*., 1989; McKenzie and Milligan, 1991). All experiments included a vehicle treatment control.

Cell culture

ST*Hdh*$^{Q7/Q7}$ and ST*Hdh*$^{Q111/Q111}$ cells are derived from the conditionally immortalized striatal progenitor cells of embryonic day 14 C57BlJ/6 mice (Coriell Institute, Camden, NJ) (Trettel *et al*., 2000). ST*Hdh*$^{Q111/Q111}$ cells express exon 1 of the mutant human *huntingtin* gene containing 111 CAG repeats knocked into the mouse *huntingtin* locus (Trettel *et al.*, 2000). ST*Hdh*$^{Q7/Q7}$ and ST*Hdh*$^{Q111/Q111}$ cells endogenously express CB_1 and dopamine D_2 receptor (Paoletti *et al*., 2008; Laprairie *et al*., 2014). Cells were maintained at 33°C, 5% CO_2 in DMEM supplemented with 10% FBS, 2 mM L-glutamine, 10^4 U mL^{-1} Pen/Strep, and 400 μg mL^{-1} geneticin. Cells were serum-deprived for 24 h prior to experiments to promote differentiation (Trettel *et al*., 2000; Laprairie *et al*., 2014).

Plasmids and transfection

Human CB_1-green fluorescent protein^2 (GFP^2) C-terminal fusion protein was generated using the $pGFP^2$-N3 (PerkinElmer, Waltham, MA) plasmid, as described previously (Bagher *et al*., 2013). Human arrestin2 (β-arrestin1)-*Renilla* luciferase II (Rluc) C-terminal fusion protein was generated using the pcDNA3.1 plasmid and

Molecular Pharmacology Fast Forward. Published on December 23, 2015 as DOI: 10.1124/mol.115.101980
This article has not been copyedited and formatted. The final version may differ from this version.

provided by Dr. Denis J Dupré (Dalhousie University, NS, CAN). The GFP^2-Rluc fusion construct, and Rluc plasmids have also been described (Bagher *et al*., 2013). The $G\alpha_q$ dominant negative mutant [Glu 209 Δ Leu, Asp 277 Δ Asn (Q209L,D277N)] pcDNA3.1 plasmid was obtained from the Missouri S&T cDNA Resource Center (Rolla, MO) (Lauckner *et al*., 2005).

Cells were grown in 6 well plates and transfected with 200 ng of the Rluc fusion plasmid and 400 ng of the GFP^2 fusion plasmid according to previously described protocols (Laprairie *et al*., 2014) using Lipofectamine 2000® according to the manufacturer's instructions (Invitrogen, Burlington, ON). Transfected cells were maintained for 48 h prior to experimentation.

Bioluminescence resonance energy transfer^2 ($BRET^2$)

Interactions between CB_1 and β-arrestin1 were quantified *via* $BRET^2$ according to previously described methods (James *et al*., 2006; Laprairie *et al*., 2014). BRET efficiency ($BRET_{Eff}$) was determined such that Rluc alone was used to calculate $BRET_{MIN}$ and the Rluc-GFP^2 fusion protein was used to calculate $BRET_{MAX}$ using previously described methods (James *et al*., 2006).

On- and In-cell™ western

On-cell™ western analyses were completed as described previously (Laprairie *et al*., 2014) using primary antibody directed against N-CB_1 (1:500; Cayman Chemical Company, Ann Arbor, MI, USA, Cat No. 101500). All experiments measuring CB_1 included an N-CB_1 blocking peptide (1:500) control, which was incubated with N-CB_1 antibody (1:500). Immunofluorescence observed with the N-CB_1 blocking peptide was subtracted from all experimental replicates. In-cell™ western analyses were conducted as

Molecular Pharmacology Fast Forward. Published on December 23, 2015 as DOI: 10.1124/mol.115.101980
This article has not been copyedited and formatted. The final version may differ from this version.

described previously (Laprairie *et al.*, 2014). Primary antibody solutions were: N-CB_1 (1:500), pERK1/2(Tyr205/185) (1:500), ERK1/2 (1:500), pCREB(S133) (1:500), CREB (1:500), pPLCβ3(S537) (1:500), PLCβ3 (1:1000), pAkt(S473) (1:500), Akt (1:1000), or β-actin (1:2000; Santa Cruz Biotechnology). Secondary antibody solutions were: $IR^{CW700dye}$ or $IR^{CW800dye}$ (1:500; Rockland Immunochemicals).

ATP quantification, γ-amino butyric acid (GABA) ELISA, and cell viability assays

The CellTiter-Glo® ATP quantification assay was used according to the manufacturer's instructions (Promega). The GABA ELISA assay was conducted according to the manufacturer's instructions for mouse cell culture media (Novatein Biosciences, Boston, MA, USA). GABA levels were reported as ΔGABA relative to GABA in vehicle-treated cells. Viability assays (calcein-AM [Cal-AM], ethidium homodimer-1 [EthD-1]) were conducted according to the manufacturer's instructions (Live/Dead Cytotoxicity Assay, Life Technologies, Burlington, ON). Cal-AM fluorescence is an indicator of cellular esterase activity and mitochondrial respiration. Cal-Am fluorescence (460/510 nm) is reported as % esterase activity relative to vehicle-treated ST*Hdh*$^{Q7/Q7}$ cells (100%). EthD-1 fluorescence is an indicator of membrane permeability and cell death. EthD-1 fluorescence (530/620 nm) is reported as % membrane permeability relative to ST*Hdh*$^{Q7/Q7}$ cells treated with 70% methanol for 30 min (100%). All measurements of viability (ATP, GABA, calcein-AM, EthD-1) were made 18 h following cannabinoid treatment.

Statistical analyses

All experiments were conducted alongside WIN as a reference ligand. While it is often considered ideal to choose the endogenous receptor agonist as a reference ligand

Molecular Pharmacology Fast Forward. Published on December 23, 2015 as DOI: 10.1124/mol.115.101980
This article has not been copyedited and formatted. The final version may differ from this version.

(Kenakin and Christopoulos, 2013), WIN was chosen as a reference ligand for these studies because 1) it is a widely used reference compound to study CB_1-dependent signalling (Lauckner *et al*., 2005), 2) it acted as an agonist in all assays with non-significant differences in EC_{50} observed between assays, and 3) we wanted determine whether the two endogenous cannabinoids, AEA and 2-AG, were inherently biased either in wild-type (ST*Hdh*$^{Q7/Q7}$) or mHtt-expressing (ST*Hdh*$^{Q111/Q111}$) cells. Concentration-response curves (CRC) for ERK, BRET^2 (CB_1/β-arrestin1), CREB, PLCβ3, and Akt are presented as % of WIN E_{max} in ST*Hdh*$^{Q7/Q7}$ cells (Griffin *et al*., 2007).

CRCs were fit to non-linear regression with variable slope (four parameter) model to determine pEC_{50} and E_{max} (Table 1), or global non-linear regression using the operational model (Black and Leff, 1983; Ehlert *et al*., 2011; Kenakin *et al*., 2011) (eq. 1) to estimate the transduction coefficient [logR (τ/K_A)], change in transducer coefficient relative to the reference ligand (ΔlogR), and bias factor (ΔΔlogR) (Prism v. 5.0, GraphPad Software Inc., San Diego, CA), as indicated. In eq. 1 E is the response, E_{max} is the maximal response, [A] is agonist concentration, n is transducer slope, τ is agonist efficacy, and K_A is the agonist's affinity for the receptor (Kenakin *et al*., 2011). In order to obtain a global least-squares fit of the data to the operational model, n was constrained to 1 and logK_A was shared between both ST*Hdh*$^{Q7/Q7}$ and ST*Hdh*$^{Q111/Q111}$ datasets and constrained to be greater than -15 (Griffin *et al.*, 2007; Ehlert, 2015). Relative activity (ΔlogR) was calculated in Prism as the difference between transduction coefficients [logR (τ/K_A)] values for two ligands, a 'test' ligand and a reference ligand (here WIN) as measured between sample-matched replicates (Kenakin *et al.*, 2011) (eq. 2). In eq. 3 Bias factor (*i.e.* log bias, ΔΔlogR) is the difference between response 1 (R_1) and response

Molecular Pharmacology Fast Forward. Published on December 23, 2015 as DOI: 10.1124/mol.115.101980
This article has not been copyedited and formatted. The final version may differ from this version.

2 (R_2) (Kenakin *et al.*, 2011). All calculations of ΔΔlogR are reported using pERK response ($G\alpha_{i/o}$) as R_1. Statistical analyses were two-way analysis of variance (ANOVA) (Prism). *Post-hoc* analyses were performed using Bonferroni's test. Homogeneity of variance was confirmed using Bartlett's test. The level of significance was set to $P < 0.01$ where ANOVA was utilized or $P < 0.05$ where non-overlapping confidence intervals (CI) were used to determine significance. Results are reported as the mean ± the standard error of the mean (SEM) from at least 4 independent experiments.

$$E = \frac{E_{max}[A]^n \tau^n}{[A]^n \tau^n + ([A] + K_A)^n} \quad \textbf{(1)}$$

$$\Delta logR = \log(\tau/K_A)_{Test\ compound} - log(\tau/K_A)_{Ref\ compound} \quad \textbf{(2)}$$

$$log\ bias = \Delta\Delta logR = \Delta\Delta\log(\tau/K_A)_{R1-R2} = \Delta log(\tau/K_A)_{R1} - \Delta log(\tau/K_A)_{R2} \quad \textbf{(3)}$$

Results

Cannabinoid-dependent signalling in the presence of mHtt.

ST*Hdh*$^{Q7/Q7}$ (Fig. 1A-E) and ST*Hdh*$^{Q111/Q111}$ (Fig. 1F-J) cells were treated with 10 nM – 10 μM WIN, CP, 2-AG, AEA, THC, CBD, or THC+CBD (1:1) and $G\alpha_{i/o}$-(ERK1/2), β-arrestin1, $G\alpha_s$- (CREB), $G\alpha_q$- (PLCβ3), and Gβγ-dependent (Akt) signalling were measured. The coupling of each of these signalling pathways to CB_1 and their respective G proteins or β-arrestin1 has been tested previously (Laprairie *et al.*, 2014) and is presented in supplementary figure 1 for a subset of cannabinoids. The agonist effects of all cannabinoids tested were CB_1-dependent, except for CBD (see below).

For pERK1/2 ($G\alpha_{i/o}$), the E_{max} observed for all cannabinoids was reduced by approximately 50% in ST*Hdh*$^{Q111/Q111}$ cells compared to ST*Hdh*$^{Q7/Q7}$ cells, with no change in pEC_{50} observed between ST*Hdh*$^{Q7/Q7}$ and ST*Hdh*$^{Q111/Q111}$ cells (Table 1; Fig.

Molecular Pharmacology Fast Forward. Published on December 23, 2015 as DOI: 10.1124/mol.115.101980
This article has not been copyedited and formatted. The final version may differ from this version.

1A,F). This is consistent with our earlier finding that the E_{max} for pERK relative to total ERK (*i.e.* raw data without reference ligand) following arachidonoyl-2'-chloroethylamide (ACEA) treatment is 50% lower in ST*Hdh*$^{Q111/Q111}$ cells expressing mHtt compared to ST*Hdh*$^{Q7/Q7}$ cells (Laprairie *et al.*, 2013). The pERK E_{max} values were greater in WIN- and AEA-treated ST*Hdh*$^{Q7/Q7}$ cells compared to 2-AG-, CP-, THC-treated ST*Hdh*$^{Q7/Q7}$ cells; CBD and THC+CBD displayed no agonist activity in ST*Hdh*$^{Q7/Q7}$ cells (Table 1; Fig. 1A). In contrast, the pERK E_{max} values were not different in 2-AG-, AEA-, WIN-, and CP-treated ST*Hdh*$^{Q111/Q111}$ cells the pERK E_{max} was lower in THC- and THC+CBD-treated ST*Hdh*$^{Q111/Q111}$ cells compared to WIN; CBD did not elicit an agonist response (Table 1; Fig. 1F). THC+CBD-treated ST*Hdh*$^{Q111/Q111}$ cells also displayed a lower pEC_{50} in the pERK assay (Table 1; Fig. 1F).

CB_1 is known to interact with β-arrestin1, which mediates receptor internalization, recycling, and degradation (Sim-Selley and Martin, 2002; Laprairie *et al.*, 2014). Unlike pERK, no differences in E_{max} and pEC_{50} were observed for β-arrestin1 assays. CP displayed higher pEC_{50} and E_{max} values than WIN, while no differences in pEC_{50} and E_{max} were observed between WIN, 2-AG and THC, and AEA displayed lower E_{max} values for β-arrestin1 recruitment in both cell lines (Table 1; Fig 1B,G). CBD was not an agonist of β-arrestin1 recruitment. In the THC+CBD-treated cells, the E_{max} and pEC_{50} of $BRET_{Eff}$ were both reduced compared to THC-treated cells (Table 1). These data are consistent with our previous finding that CBD is a negative allosteric modulator of THC-dependent effects at CB_1 (Laprairie *et al.*, 2015).

The observed E_{max} and pEC_{50} for pCREB ($G\alpha_S$) was not different in ST*Hdh*$^{Q7/Q7}$ cells treated with WIN, CP, CBD, or THC+CBD, relative to ST*Hdh*$^{Q111/Q111}$ cells (Table

Molecular Pharmacology Fast Forward. Published on December 23, 2015 as DOI: 10.1124/mol.115.101980
This article has not been copyedited and formatted. The final version may differ from this version.

1; Fig 1C,H). AEA and 2-AG did not evoke a pCREB response. CP, CBD, and THC+CBD treatment resulted in higher E_{max} values for pCREB than WIN treatment in both cell lines. pCREB pEC_{50} and E_{max} values were higher in CP- and CBD-treated cells compared to THC+CBD-treated cells (Table 1; Fig. 1C,H). Because CB_1-dependent $G\alpha_S$ signalling is uncommon, this was examined further (see below).

CB_1 can also couple $G\alpha_q$ to modulate Ca^{2+}- and PLCβ3-dependent signalling (Lauckner *et al*., 2005). No differences were observed for PLCβ3 phosphorylation between ST*Hdh*$^{Q7/Q7}$ and ST*Hdh*$^{Q111/Q111}$ cells (Table 1; Fig 1D,I). pPLCβ3 E_{max} values were greater in WIN-, 2-AG-, and AEA-treated cells compared to CP- and THC-treated cells, with no change in pEC_{50} (Table 1; Fig 1D,I). CBD was not an agonist of PLCβ3 phosphorylation.

In the case of pAkt (Gβγ), no differences were observed between ST*Hdh*$^{Q7/Q7}$ and ST*Hdh*$^{Q111/Q111}$ cells (Table 1; Fig 1E,J). pAkt E_{max} values were greater in WIN-, 2-AG-, and AEA-treated cells compared to CP-treated cells, which were in turn greater compared to THC-treated cells (Table 1; Fig 1E,J). pAkt pEC_{50} values did not differ between agonists. CBD was not an agonist of Akt phosphorylation.

Operational model analysis of cannabinoid transduction coefficients (logR) and relative activity (Δ logR) in the presence of mHtt.

The operational model global non-linear regression (eq. 1) was used to analyze concentration-response data for cannabinoid signalling bias in ST*Hdh*$^{Q7/Q7}$ and ST*Hdh*$^{Q111/Q111}$ cells. CBD only displayed agonist activity for pCREB and these data were therefore omitted from global non-linear regression analyses of pERK, β-arrestin1, pPLCβ3, and pAkt assays. The transduction coefficient [logR (τ/ K_A)] for the ERK

Molecular Pharmacology Fast Forward. Published on December 23, 2015 as DOI: 10.1124/mol.115.101980
This article has not been copyedited and formatted. The final version may differ from this version.

response was lower in THC- and THC+CBD-treated cells compared to WIN-treated cells, and was lower in THC- and THC+CBD-treated ST*Hdh*$^{Q111/Q111}$ cells compared to ST*Hdh*$^{Q7/Q7}$ cells (Table 2). logR for β-arrestin1 was also lower in THC- (only ST*Hdh*$^{Q111/Q111}$) and THC+CBD-treated cells compared to WIN-treated cells, was lower in THC- and THC+CBD-treated ST*Hdh*$^{Q111/Q111}$ cells compared to ST*Hdh*$^{Q7/Q7}$ cells, and was higher in THC- and THC+CBD-treated cells compared to the ERK response (Table 2). logR for the CREB response was higher in CP-treated cells, and lower in THC+CBD-treated cells, compared to WIN, was lower in WIN-treated ST*Hdh*$^{Q111/Q111}$ cells compared to ST*Hdh*$^{Q7/Q7}$ cells, and was lower in WIN-treated cells compared to the ERK response (Table 2). logR for the PLCβ3 response was lower in CP- (only ST*Hdh*$^{Q7/Q7}$), AEA-, THC-, and THC+CBD-treated cells, compared to WIN, was lower in CP-, AEA-, and THC-treated ST*Hdh*$^{Q111/Q111}$ cells compared to ST*Hdh*$^{Q7/Q7}$ cells, and was lower in AEA- and THC-treated cells compared to the ERK response (Table 2). Finally, logR for the Akt response was lower in CP-, THC-, and THC+CBD-treated cells, was lower in THC- and THC+CBD-treated ST*Hdh*$^{Q111/Q111}$ cells compared to ST*Hdh*$^{Q7/Q7}$ cells, and was lower in THC-treated ST*Hdh*$^{Q7/Q7}$ cells compared to the ERK response (Table 2).

Relative activity (ΔlogR) was calculated using WIN as the reference ligand (eq. 2). WIN was chosen as a reference ligand, rather than the endocannabinoids 2-AG and AEA (Kenakin and Christopoulos, 2013), because it displayed activity in all assays and we wanted to quantify the relative activity and bias of 2-AG and AEA in ST*Hdh*$^{Q7/Q7}$ and ST*Hdh*$^{Q111/Q111}$ cells. The ΔlogR for ERK response was lower in THC- and THC+CBD-treated cells compared to WIN (ΔlogR = 0) (Table 2). The ΔlogR for β-arrestin1 was lower in 2-AG, AEA, THC- and THC+CBD-treated cells compared to WIN, and

Molecular Pharmacology Fast Forward. Published on December 23, 2015 as DOI: 10.1124/mol.115.101980
This article has not been copyedited and formatted. The final version may differ from this version.

compared to the ERK response (Table 2). The ΔlogR for β-arrestin1 was lower in THC-treated ST*Hdh*$^{Q111/Q111}$ cells, and higher in THC+CBD-treated ST*Hdh*$^{Q111/Q111}$ cells, compared to ST*Hdh*$^{Q7/Q7}$ cells (Table 2). The ΔlogR for the CREB response was higher in CP- (both cell types) and THC+CBD- treated ST*Hdh*$^{Q111/Q111}$ cells, and lower in THC+CBD-treated ST*Hdh*$^{Q7/Q7}$ cells, compared to WIN (Table 2). The ΔlogR for the CREB response was higher in CP- (both cell types) and THC+CBD-treated ST*Hdh*$^{Q111/Q111}$ cells compared to the ERK response, and was greater in THC+CBD-treated ST*Hdh*$^{Q111/Q111}$ cells compared to ST*Hdh*$^{Q7/Q7}$ cells (Table 2). The ΔlogR for the PLCβ3 response was lower in CP- (only ST*Hdh*$^{Q7/Q7}$), 2-AG- (only ST*Hdh*$^{Q7/Q7}$), AEA- (only ST*Hdh*$^{Q111/Q111}$), THC- and THC+CBD-treated cells compared to WIN, and compared to the ERK response for CP, 2-AG, and AEA treatments (Table 2). The ΔlogR for the PLCβ3 response was lower in THC- and THC+CBD-treated ST*Hdh*$^{Q111/Q111}$ cells compared to ST*Hdh*$^{Q7/Q7}$ cells (Table 2). Finally, the ΔlogR for the Akt response was lower in CP- (only ST*Hdh*$^{Q7/Q7}$), AEA- (only ST*Hdh*$^{Q7/Q7}$), THC-, and THC+CBD-treated cells compared to WIN, and compared to the ERK response for CP and THC (Table 2). ΔlogR values for the Akt response were lower and higher in THC- and THC+CBD-treated ST*Hdh*$^{Q111/Q111}$ cells, respectively, compared to ST*Hdh*$^{Q7/Q7}$ cells (Table 2).

Summarizing the data in table 2 we observed that the rank order of τ/K_A and relative activity (ΔlogR) for pERK was AEA > WIN > CP (ST*Hdh*$^{Q7/Q7}$) > 2-AG > CP (ST*Hdh*$^{Q111/Q111}$) > THC ≥ THC+CBD. For β-arrestin1 this order was CP > THC ≥ WIN > 2-AG = AEA > THC (ST*Hdh*$^{Q111/Q111}$) > THC+CBD. For pCREB this order was CP > WIN (ST*Hdh*$^{Q7/Q7}$) > CBD (ST*Hdh*$^{Q7/Q7}$) > THC+CBD (ST*Hdh*$^{Q111/Q111}$) > CBD (ST*Hdh*$^{Q111/Q111}$) > WIN (ST*Hdh*$^{Q111/Q111}$) ≥ THC+CBD (ST*Hdh*$^{Q7/Q7}$). For pPLCβ3 the

Molecular Pharmacology Fast Forward. Published on December 23, 2015 as DOI: 10.1124/mol.115.101980
This article has not been copyedited and formatted. The final version may differ from this version.

order was WIN > CP (ST*Hdh*$^{Q111/Q111}$) > AEA (ST*Hdh*$^{Q7/Q7}$) > 2-AG (ST*Hdh*$^{Q7/Q7}$) > CP (ST*Hdh*$^{Q7/Q7}$) > 2-AG (ST*Hdh*$^{Q7/Q7}$) > THC (ST*Hdh*$^{Q7/Q7}$) > AEA (ST*Hdh*$^{Q7/Q7}$) > THC (ST*Hdh*$^{Q7/Q7}$) > THC+CBD. And for pAkt the order was AEA ≥ 2-AG = WIN > CP > THC > THC+CBD.

Operational model analysis of cannabinoid-dependent system bias (ΔΔlogR) in the presence of mHtt.

Bias values (ΔΔlogR) were calculated from the relative activity data (ΔlogR) in order to characterize functional selectivity in ST*Hdh*$^{Q7/Q7}$ and ST*Hdh*$^{Q111/Q111}$ cells (eq. 3) (Fig. 2A-D). Because CB_1 is classically considered a $G\alpha_{i/o}$-coupled receptor (Kondo *et al.*, 1998; Lauckner *et al.*, 2005), all comparisons were made using $G\alpha_{i/o}$-dependent ERK1/2 signalling (pERK) as $\Delta\log R_1$. Based on these data, CP evoked $G\alpha_S$- and β-arrestin1-biased signalling compared to $G\alpha_{i/o}$, and $G\alpha_{i/o}$-biased signalling compared to $G\alpha_q$ or Gβγ in both cell types tested here (*i.e.* $G\alpha_S$ > β-arrestin1 > $G\alpha_{i/o}$ > $G\alpha_q$ > Gβγ) (Fig. 2A-D). 2-AG evoked $G\alpha_{i/o}$-biased signalling compared to β-arrestin1 (in ST*Hdh*$^{Q7/Q7}$ cells) and $G\alpha_q$ (more so in ST*Hdh*$^{Q111/Q111}$ cells), and Gβγ-biased signalling compared to $G\alpha_{i/o}$ (in ST*Hdh*$^{Q7/Q7}$ cells) (*i.e.* Gβγ > $G\alpha_{i/o}$ > β-arrestin1 > $G\alpha_q$) (Fig. 2A-D). Like 2-AG, AEA evoked $G\alpha_{i/o}$-biased signalling compared to β-arrestin1 and $G\alpha_q$ (more so in ST*Hdh*$^{Q111/Q111}$ cells), and Gβγ-biased signalling compared to $G\alpha_{i/o}$ (in ST*Hdh*$^{Q7/Q7}$ cells) (*i.e.* Gβγ > $G\alpha_{i/o}$ > β-arrestin1 > $G\alpha_q$) (Fig. 2A-D). THC evoked β-arrestin1-, $G\alpha_q$-, and Gβγ-biased signalling compared to $G\alpha_{i/o}$, in both cell types (*i.e.* β-arrestin1 > $G\alpha_q$ = Gβγ > $G\alpha_{i/o}$) (Fig. 2A-D). CBD treatment only produced a significant activation of $G\alpha_S$-dependent CREB phosphorylation and bias values could not be calculated for this ligand. The combination THC+CBD evoked $G\alpha_S$-biased signalling compared to $G\alpha_{i/o}$ and $G\alpha_{i/o}$-

Molecular Pharmacology Fast Forward. Published on December 23, 2015 as DOI: 10.1124/mol.115.101980
This article has not been copyedited and formatted. The final version may differ from this version.

biased signalling compared to β-arrestin1, $G\alpha_q$, or Gβγ (more so in ST*Hdh*$^{Q7/Q7}$ cells) (*i.e.* $G\alpha_S > G\alpha_{i/o} >$ β-arrestin1 = $G\alpha_q$ = Gβγ) (Fig. 2A-D).

Each cannabinoid analyzed here displayed unique functional selectivity for different signalling pathways. Overall, the bias factor of 2-AG and AEA was shifted toward $G\alpha_{i/o}$-dependent ERK phosphorylation, and the bias factor of THC+CBD was shifted away from $G\alpha_{i/o}$-dependent ERK phosphorylation, in ST*Hdh*$^{Q111/Q111}$ cells. The reduced pERK E_{max} in mHtt-expressing ST*Hdh*$^{Q111/Q111}$ cells compared to ST*Hdh*$^{Q7/Q7}$ cells (Table 1) may result from lower CB_1 levels (50%) (Laprairie *et al.*, 2013). An important advantage of using the operational model to estimate the relative activity and ligand bias is that this model negates the effects of differences in receptor density (Kenakin *et al*., 2011). Therefore, differences in bias between ST*Hdh*$^{Q7/Q7}$ and ST*Hdh*$^{Q111/Q111}$ cells were likely mHtt-dependent and not the result of changes in agonist potency or efficacy.

Cannabinoid-specific changes in cellular function and viability.

Treatment of ST*Hdh*$^{Q7/Q7}$ cells with WIN, 2-AG, AEA, or THC resulted in a small increase in ATP, whereas treatment with CP, CBD, or THC+CBD resulted in a decrease in ATP (Fig. 3A). In ST*Hdh*$^{Q111/Q111}$ cells, basal ATP levels were approximately 50% lower than basal ATP levels in ST*Hdh*$^{Q7/Q7}$ cells. ATP levels increased in ST*Hdh*$^{Q111/Q111}$ cells treated with WIN, 2-AG, AEA, or THC and decreased with CP or CBD (Fig. 3E). THC+CBD treatment resulted in higher ATP levels in ST*Hdh*$^{Q111/Q111}$ cells. CP and CBD were the only cannabinoids tested that evoked $G\alpha_S$-biased (CREB) signalling in ST*Hdh* cells. The lower ATP levels observed in cells treated with CP or CBD may have resulted from cAMP production. However, given that cells expressing mHtt are deficient in ATP

Molecular Pharmacology Fast Forward. Published on December 23, 2015 as DOI: 10.1124/mol.115.101980
This article has not been copyedited and formatted. The final version may differ from this version.

(Sadri-Vakili *et al.*, 2006; Laprairie *et al.*, 2013), cannabinoids that exaggerate this state may exacerbate cellular pathology.

Excessive glutamate release from cortical neurons and GABA release from striatal medium spiny projection neurons are both observed in HD (Benn *et al.*, 2007; Botelho *et al.*, 2014). Compounds that limit neurotransmitter release may, therefore, be beneficial in HD, whereas compounds that enhance neurotransmitter release may exacerbate HD pathophysiology. GABA release was inhibited by WIN, 2-AG, AEA, CP, and THC in ST*Hdh*$^{Q7/Q7}$ and ST*Hdh*$^{Q111/Q111}$ cells (Fig. 3B,F). CBD treatment was associated with enhanced GABA release in ST*Hdh*$^{Q7/Q7}$ and ST*Hdh*$^{Q111/Q111}$ cells and the EC_{50} and E_{max} of this response were reduced in the presence of THC (THC+CBD) (Fig. 3B,F). Therefore, CBD treatment may enhance excessive neurotransmitter release in HD, whereas other cannabinoids tested here limited neurotransmitter release.

Cell viability was measured by cal-AM fluorescence, which is an indicator of esterase activity and mitochondrial respiration that is positively correlated with viability, and EthD-1 fluorescence, which is an indicator of membrane permeability and cell death and therefore negatively correlated with viability (MacCoubrey *et al.*, 1990). Basal cal-AM fluorescence (% esterase activity) was 60% less in ST*Hdh*$^{Q111/Q111}$ cells compared to ST*Hdh*$^{Q7/Q7}$ cells (Fig. 3C,G). Cal-AM fluorescence was decreased by 40% in ST*Hdh*$^{Q7/Q7}$ and ST*Hdh*$^{Q111/Q111}$ cells treated with CP or THC and increased by 40% in ST*Hdh*$^{Q111/Q111}$ cells treated with WIN, 2-AG, AEA, or CBD (Fig. 3C,G). Basal EthD-1 fluorescence (% membrane permeable cells) was 40% greater in ST*Hdh*$^{Q111/Q111}$ cells compared to ST*Hdh*$^{Q7/Q7}$ cells (Fig. 3D,H). EthD-1 fluorescence was increased by 30% in ST*Hdh*$^{Q7/Q7}$ and ST*Hdh*$^{Q111/Q111}$ cells treated with CP or THC (Fig. 3D,H). EthD-1

Molecular Pharmacology Fast Forward. Published on December 23, 2015 as DOI: 10.1124/mol.115.101980
This article has not been copyedited and formatted. The final version may differ from this version.

fluorescence was decreased by 20% in AEA- and CBD-treated ST*Hdh*$^{Q7/Q7}$ cells, and by 40% in WIN-, 2-AG-, AEA-, and CBD-treated ST*Hdh*$^{Q111/Q111}$ cells (Fig. 3D,H). The effect of CBD predominated over that of THC for both cal-AM and EthD-1 fluorescence in both cell lines. Therefore, in these viability assays, the CP and THC (which both displayed β-arrestin1 bias) appeared harmful whereas other cannabinoids improved viability in ST*Hdh*$^{Q111/Q111}$ cells.

Functional CB_1 residing at the plasma membrane undergo internalization following ligand binding and β-arrestin recruitment (Blair *et al*., 2009). Total CB_1 levels were higher in WIN-, 2-AG-, and AEA-treated ST*Hdh*$^{Q7/Q7}$ and ST*Hdh*$^{Q111/Q111}$ cells, compared to vehicle, while total CB_1 levels were lower in CP- and THC-treated ST*Hdh*$^{Q7/Q7}$ and ST*Hdh*$^{Q111/Q111}$ cells (Fig. 4A). The fraction of CB_1 at the plasma membrane and total CB_1 was assayed in ST*Hdh*$^{Q7/Q7}$ and ST*Hdh*$^{Q111/Q111}$ cells treated with various cannabinoids for 12 h (Fig. 4A,B). The fraction of CB_1 at the plasma membrane was lower in WIN-, 2-AG-, CP-, and THC-treated cells, and higher in CBD-treated cells (Fig. 4B). CP and THC – and to a lesser extent WIN and 2-AG – displayed greater β-arrestin1 bias than AEA or CBD. The mechanism of cannabinoid-dependent induction of CB_1 expression has been described previously (Laprairie *et al*., 2013). Here, it is important to note that treatment with cannabinoids that evoked $G\alpha_{i/o}$-and $G\beta\gamma$-biased signalling (2-AG, AEA) was associated with higher CB_1 levels, whereas treatment with CP and THC (β-arrestin1-biased cannabinoids) was associated with lower CB_1 levels, suggesting that cannabinoids that are functionally selective for β-arrestin1 may reduce the available pool of CB_1 receptors. The effects of THC and CBD were neutralized by one another (Fig. 4A,B).

Molecular Pharmacology Fast Forward. Published on December 23, 2015 as DOI: 10.1124/mol.115.101980
This article has not been copyedited and formatted. The final version may differ from this version.

Mechanism of CP- and CBD-dependent $G\alpha_S$ signalling.

CBD is known to modulate the activity of many cellular GPCRs, including CB_1, the type 2 cannabinoid receptor (CB_2) (Hayakawa *et al*., 2008), the serotonin $5HT_{1A}$ receptor (Russo *et al*., 2005), GPR55 (Ryberg *et al*., 2007), and the μ- and δ-opioid receptors (Kathmann *et al*., 2006). Here, CBD treatment resulted in CB_1-independent CREB phosphorylation (Fig. 5). CREB phosphorylation was highest 30 min after CBD treatment and was sustained for the duration of the experiment (60 min) (Fig. 5A). Treatment of ST*Hdh*$^{Q7/Q7}$ cells with the $5HT_{1A}$ agonist 8-OH-DPAT resulted in a dose-dependent increase in CREB phosphorylation that was competitively inhibited by the $5HT_{1A}$ antagonist WAY 100635 and CBD (Fig. 5B). Treatment of ST*Hdh*$^{Q7/Q7}$ cells with CBD alone also resulted in a dose-dependent increase in CREB phosphorylation, with less potency and efficacy that the full agonist 8-OH-DPAT (Fig. 5C). CBD-dependent CREB phosphorylation was not inhibited by the CB_1 antagonist O-2050, but was inhibited by WAY 100635 (Fig. 5C), indicating that CBD activated CREB *via* $5HT_{1A}$. It is not known whether the partial agonism of $5HT_{1A}$ by CBD is functionally antagonistic of serotonergic signalling *in vivo* and whether this would play a role in CBD-based treatments of neurological disorders.

Unexpectedly, we observed a switch in signalling following continued drug exposure for CP. At 10 min CP treatment produced $G\alpha_{i/o}$-dependent ERK phosphorylation that returned to basal levels by 25 min; and at 30 min CP treatment produced $G\alpha_s$-dependent CREB phosphorylation (Fig. 5A). ST*Hdh* cells endogenously express D_2 (Paoletti *et al.*, 2008) and heterodimerization of CB_1 and D_2 is known to lead to a switch in coupling *from* $G\alpha_{i/o}$ *to* $G\alpha_s$ following treatment with CP (Glass and Felder,

Molecular Pharmacology Fast Forward. Published on December 23, 2015 as DOI: 10.1124/mol.115.101980
This article has not been copyedited and formatted. The final version may differ from this version.

1997; Kearn *et al.*, 2005). Therefore, we hypothesized that CP could be functionally selective for CB_1/D_2 heterodimer signalling to explain the switch from $G\alpha_{i/o}$ to $G\alpha_s$. Co-treatment of ST*Hdh*$^{Q7/Q7}$ cells with CP and 1 μM quinpirole (a D_2 agonist) shifted the concentration-response curve for CREB phosphorylation right, as did co-treatment with O-2050 (a competitive antagonist of CB_1), while co-treatment with 10 μM haloperidol (a D_2 antagonist) shifted the concentration-response curve left (Fig. 5D). Quinpirole and haloperidol did not effect CREB phosphorylation alone (Fig. 5D). From these data, we suggest that CP selectively enhanced either physical heterodimerization between CB_1/D_2 or functional signalling through these receptors with a subsequent switch from $G\alpha_{i/o}$ *to* $G\alpha_s$ (Kearn *et al.*, 2005).

Discussion

Correlations between functional selectivity and cellular viability

In this study, we described the biased signalling properties of 6 cannabinoids in the ST*Hdh* cell culture model of striatal medium spiny projection neurons. System bias shifted toward $G\alpha_{i/o}$ for 2-AG and AEA in ST*Hdh*$^{Q111/Q111}$ cells (mHtt-expressing) cells compared to ST*Hdh*$^{Q7/Q7}$ cells. Treatment of ST*Hdh*$^{Q111/Q111}$ cells with cannabinoids that signalled *via* CB_1 and were functionally selective for $G\alpha_{i/o}$ and $G\beta\gamma$ (2-AG, AEA) was associated with the greatest improvement in ATP production, inhibition of GABA release, cellular metabolic activity (esterase activity), and cell death (membrane permeability). In contrast, ligands that preferentially enhanced β-arrestin1-recruitment (THC and CP) reduced cellular viability in both ST*Hdh*$^{Q7/Q7}$ and ST*Hdh*$^{Q111/Q111}$ cells as determined by the same measures. We have previously observed that derivatives of AEA normalize CB_1

Molecular Pharmacology Fast Forward. Published on December 23, 2015 as DOI: 10.1124/mol.115.101980
This article has not been copyedited and formatted. The final version may differ from this version.

levels in ST*Hdh*$^{Q111/Q111}$ cells *via* $G\alpha_{i/o}$, $G\beta\gamma$, Akt, and NF-κB and that normalization of CB_1 was associated with improved cell function and viability (Laprairie *et al*., 2013, 2014). Recently, three studies have demonstrated that increasing CB_1 levels in medium spiny projection neurons in the R6/2 mouse model of HD *via* adenovirus-mediated overexpression normalizes brain-derived neurotrophic factor levels, reduces striatal atrophy and prevents decreases in dendritic spine density and levels of excitatory synaptic markers such as synaptophysin and vesicular glutamate transporter, but does not improve deficits in motor coordination (Chiarlone *et al*., 2014; Naydenov *et al*., 2014; Blázquez *et al*., 2015). In accordance with this, knockdown or knockout of CB_1 in medium spiny projection neurons of R6/2, N171-82Q, or *Hdh*$^{Q150/Q150}$ HD mice further reduces the pool of CB_1 and exacerbates deficits in motor control, enhances striatal atrophy, reduces survival (Blázquez *et al*., 2011; Mievis *et al*., 2011; Horne *et al*., 2013). Further, individuals with HD and a variant of the CB_1 gene (*CNR1* rs4707436), that is associated with lower levels of CB_1, begin displaying motor-related symptoms of HD earlier than individuals with HD and normal *CNR1* (Kloster *et al*., 2013). Together, these studies and our data provide support for $G\alpha_{i/o}$- and $G\beta\gamma$-selective activation of CB_1 in order to maintain CB_1 levels and the cellular function and viability of cells expressing mHtt (Blázquez *et al*., 2011, 2015; Mievis *et al*., 2011; Horne *et al*., 2013; Chiarlone *et al*., 2014; Naydenov *et al*., 2014).

Use of THC and CBD in HD

Despite a lack of clinical evidence, patients suffering from HD may be seeking medical marijuana or acquiring it from other sources in an attempt to relieve some of the symptoms of their disease (Müller-Vahl *et al*., 1999; Meisel and Friedman, 2012; Koppel

Molecular Pharmacology Fast Forward. Published on December 23, 2015 as DOI: 10.1124/mol.115.101980
This article has not been copyedited and formatted. The final version may differ from this version.

et al., 2014). Most medically available and tested illicit marijuana contains a high concentration of THC relative to other cannabinoids, such as CBD (De Backer *et al.*, 2012). Here, we observed that THC reduced cellular function and viability in cells expressing mHtt whether THC was used alone or in a 1:1 combination with CBD. Similarly, treatment of R6/1 and R6/2 mouse models with 10 mg/kg THC is associated with worsening of HD signs and symptoms (Dowie *et al.*, 2010). However, others have reported improvement in motor control and reduced striatal atrophy in R6/1 and R6/2 HD treated for 6 weeks with 2 mg/kg THC beginning at 4 weeks of age (Blázquez *et al.*, 2011), suggesting that the deleterious effects of THC in HD are dose- and time course-dependent. CBD alone displayed mixed beneficial and negative effects in ST*Hdh*$^{Q7/Q7}$ and ST*Hdh*$^{Q111/Q111}$ cells. CBD is known to act through a number of effectors, including as a negative allosteric modulator at CB_1 and a partial agonist at $5HT_{1A}$ (Pazos *et al.*, 2013; Laprairie *et al*., 2015). It is unclear which effects of CBD predominate *in vivo* normally and in HD and how the combinations of any or all of the at least 65 cannabinoids found in marijuana (McPartland *et al.*, 2015) influence one another's pharmacokinetics and pharmacodynamics (Sagredo *et al.*, 2011; Valdeolivas *et al*., 2012). Further, the utility of CBD in HD remains controversial, with some studies reporting no effects in animal models and human trials (Consroe *et al*., 1991; Valdeolivas *et al*., 2012), or positive effects in animal models (Sagredo *et al*., 2007, 2011). Overall, the use of THC or marijuana may exacerbate the signs and symptoms of HD *via* further downregulation of CB_1 and reduced cellular viability.

Molecular Pharmacology Fast Forward. Published on December 23, 2015 as DOI: 10.1124/mol.115.101980
This article has not been copyedited and formatted. The final version may differ from this version.

Conclusions

$G\alpha_{i/o}$- and $G\beta\gamma$-selective CB_1 ligands are likely to be the most therapeutically useful cannabinoids in the treatment of HD. However, highly potent synthetic cannabinoids, such as WIN, may produce unwanted psychoactive effects and their chronic use is likely to result in receptor desensitization or downregulation (Sim-Selley and Martin, 2002; Blair *et al*., 2009). Endocannabinoids, which we observed to enhance $G\alpha_{i/o}$- and $G\beta\gamma$-dependent signalling in the ST*Hdh* cell culture system, are rapidly metabolized *in vivo* and consequently have limited efficacy when they are directly administered (Devane *et al.,* 1992; Kondo *et al*., 1998). The inhibitor of endocannabinoid catabolism URB597 has demonstrated limited efficacy at improving motor control deficits in R6/2 HD mice (Dowie *et al.*, 2010), but additional studies are needed to understand how elevating endocannabinoid levels affects the signs and symptoms of HD *in vivo*. An alternative means of enhancing endogenous CB_1 signalling is with the use of positive allosteric modulators (PAMs) of CB_1. PAMs bind to a site on the receptor that is distinct from the site of endogenous ligand binding (*i.e.* the orthosteric site) and enhance the binding and efficacy of the endogenous ligands that are produced and regulated through intrinsic control mechanisms (Pamplona *et al*., 2012; Wootten *et al*., 2013). CB_1 PAMs are more likely to increase $G\alpha_{i/o}$ and pro-survival endocannabinoids and less likely to produce the psychotropic effects associated with cannabinoid agonists because they are unable to directly activate CB_1. Our *in vitro* study of cannabinoid functional selectivity leads us to conclude that enhancement of endocannabinoid-dependent CB_1 activation is the most likely means of treating the signs of symptoms of HD by targeting CB_1.

Molecular Pharmacology Fast Forward. Published on December 23, 2015 as DOI: 10.1124/mol.115.101980
This article has not been copyedited and formatted. The final version may differ from this version.

Acknowledgements

We thank Drs. Laura Bohn and Edward Stahl for their assistance and consultation in reviewing the data presented here.

Authorship Contributions

Participated in research design: Laprairie, Bagher, Kelly, and Denovan-Wright.

Conducted experiments: Laprairie.

Contributed new reagents or analytic tools: Kelly and Denovan-Wright.

Performed data analysis: Laprairie and Denovan-Wright.

Wrote or contributed to the writing of the manuscript: Laprairie, Bagher, Kelly, and Denovan-Wright

Molecular Pharmacology Fast Forward. Published on December 23, 2015 as DOI: 10.1124/mol.115.101980
This article has not been copyedited and formatted. The final version may differ from this version.

References

Bagher AM, Laprairie RB, Kelly ME, and Denovan-Wright EM (2013) Co-expression of the human cannabinoid receptor coding region splice variants (hCB_1) affects the function of hCB_1 receptor complexes. *Eur J Pharmacol* **721**: 341–354**.**

Benn CL, Slow EJ, Farrell LA, Graham R, Deng Y, Hayden MR, and Cha JH (2007) Glutamate receptor abnormalities in the YAC128 transgenic mouse model of Huntington's disease. *Neuroscience* **147**: 354–372.

Black JW and Leff P (1983) Operational models of pharmacological agonism. *Proc Roy Soc London B* **220**: 141–162.

Blair RE, Deshpande LS, Sombati S, Elphick MR, Martin BR, and DeLorenzo RJ (2009) Prolonged exposure to WIN causes downregulation of the CB1 receptor and the development of tolerance to its anticonvulsant effects in the hippocampal neuronal culture model of acquired epilepsy. *Neuropharmacology* **57**: 208–218.

Blázquez C, Chiarlone A, Sagredo O, Aguado T, Pazos MR, Resel E, Palazuelos J, Julien B, Salazar M, Börner C, Benito C, Carrasco C, Diez-Zaera M, Paoletti P, Díaz-Hernández M, Ruiz C, Sendtner M, Lucas JJ, de Yébenes JG, Marsicano G, Monory K, Lutz B, Romero J, Alberch J, Ginés S, Kraus J, Fernández-Ruiz J, Galve-Roperh I, and Guzmán M (2011) Loss of striatal type 1 cannabinoid receptors is a key pathogenic factor in Huntington's disease. *Brain* **134**: 119–136.

Blázquez C, Chiarlone A, Bellocchio L, Resel E, Pruunsild P, García-Rincón D, Sendtner M, Timmusk T, Lutz B, Galve-Roperh I, and Guzmán M (2015) The CB1 cannabinoid receptor signals striatal neuroprotection via a PI3K/Akt/mTORC1/BDNF pathway. *Cell Death Differ* **22**: 1618–1629.

Botelho EP, Wang E, Chen JY, Holley S, Andre V, Cepeda C, and Levine MS (2014) Differential Synaptic and Extrasynaptic Glutamate-Receptor Alterations in Striatal Medium-Sized Spiny Neurons of Aged YAC128 Huntington's Disease Mice. *PLoS Curr* **6**: doi 10.1371.

Chiarlone A, Bellocchio L, Blázquez C, Resel E, Soria-Gómez E, Cannich A, Ferrero JJ, Sagredo O, Benito C, Romero J, Sánchez-Prieto J, Lutz B, Fernández-Ruiz J, Galve-Roperh I, and Guzmán M (2014) A restricted population of CB1 cannabinoid receptors with neuroprotective activity. *Proc Natl Acad Sci U S A* **111**: 8257–8262.

Christopoulos A (2014) Advances in G protein-coupled receptor allostery: from function to structure. *Mol Pharmacol* **86**: 463–478.

Consroe P, Laguna J, Allender J, Snider S, Stern L, Sandyk R, Kennedy K, and Schram K (1991) Controlled clinical trial of cannabidiol in Huntington's disease. *Pharmacol Biochem Behav* **40**: 701–708.

De Backer B, Maebe K, Verstraete AG, and Charlier C (2012) Evolution of the content of THC and other major cannabinoids in drug-type cannabis cuttings and seedlings during growth of plants. *J Forensic Sci* **57**: 918–922.

Devane WA, Hanus L, Breuer A, Pertwee RG, Stevenson LA, Griffin G, Gibson D, Mandelbaum A, Etinger A, and Mechoulam R (1992) Isolation and structure of a brain constituent that binds to the cannabinoid receptor. *Science* **258**: 1946–1949.

Denovan-Wright EM and Robertson HA (2000) Cannabinoid receptor messenger RNA levels decrease in a subset of neurons of the lateral striatum, cortex and hippocampus of transgenic Huntington's disease mice. *Neuroscience* **98**: 705– 713.

Dowie MJ, Howard ML, Nicholson LF, Faull RL, Hannan AJ, and Glass M (2010) Behavioural and molecular consequences of chronic cannabinoid treatment in Huntington's disease transgenic mice. *Neuroscience* **170**: 324–336.

Dupré DJ, Thompson C, Chen Z, Rollin S, Larrivée JF, Le Gouill C, Rola-Pleszczynski M, and Stanková J (2007) Inverse agonist-induced signalling and down-regulation of the platelet-activating factor receptor. *Cell Signal* **19**: 2068–2079.

Ehlert RJ (2015) Functional studies cast light on receptor states. *Trends Pharmacol Sci* **36**: 596–604.

Ehlert FJ, Suga H, and Griffin MT (2011) Quantifying agonist activity at G protein-coupled receptors. *J Vis Exp* **58**: e3179.

Fernández-Ruiz J (2009) The endocannabinoid system as a target for the treatment of motor dysfunction. *Br J Pharmacol* **156**: 1029–1040.

Glass M and Felder CC (1997) Concurrent stimulation of cannabinoid CB1 and dopamine D2 receptors augments cAMP accumulation in striatal neurons: evidence for a Gs linkage to the CB1 receptor. *J Neurosci* 17: 5327–5333.

Glass M, Dragunow M, and Faull RL (2000) The pattern of neurodegeneration in Huntington's disease: a comparative study of cannabinoid, dopamine, adenosine and GABA(A) receptor alterations in the human basal ganglia in Huntington's disease. *Neuroscience* **97**: 505–519.

Griffin MT, Figueroa KW, Liller S, and Ehlert FJ (2007) Estimation of agonist activity a G protein-coupled receptors: analysis of M2 muscarinic receptor signaling through Gi/o, Gs, and G15. *J Pharmacol Exp Ther* **321**: 1193–1207.

Hayakawa K, Mishima K, Irie K, Hazekawa M, Mishima S, Fujioka M, Orito K, Egashira N, Katsurabayashi S, Takasaki K, Iwasaki K, and Fujiwara M (2008) Cannabidiol prevents a post-ischemic injury progressively induced by cerebral ischemia via a high-mobility group box1-inhibiting mechanism. *Neuropharmacol* **55**: 1280–1286.

Horne EA, Coy J, Swinney K, Fung S, Cherry AE, and Marrs WR (2013) Downregulation of cannabinoid receptor 1 from neuropeptide Y interneurons in the basal ganglia of patients with Huntington's disease and mouse models. *Eur J Neurosci* **37**: 429–440.

James JR, Oliveira MI, Carmo AM, Iaboni A, and Davis SJ (2006) A rigorous experimental framework for detecting protein oligomerization using bioluminescence resonance energy transfer. *Nat Methods* **3**: 1001–1006.

Kathmann M, Flau K, Redmer A, Tränkle C, and Schlicker E (2006) Cannabidiol is an allosteric modulator at mu- and delta-opioid receptors. *Naunyn Schmiedebergs Arch Pharmacol* **372**: 354–361.

Kearn CS, Blake-Palmer K, Daniel E, Mackie K, and Glass M (2005) Concurrent stimulation of cannabinoid CB1 and dopamine D2 receptors enhances heterodimer formation: a mechanism for receptor cross-talk? *Mol Pharmacol* **67**: 1697–1704.

Kenakin T, Watson C, Muniz-Medina V, Christopoulos A, and Novick S (2011) A simple method for quantifying functional selectivity and agonist bias. *ACS Chem Neurosci* **3**: 193–203.

Kenakin T and Christopoulos A (2013) Measurements of ligand bias and functional selectivity. *Nat Rev Drug Discov* **12**: 483.

Khajehali E, Malone DT, Glass M, Sexton PM, Christopoulos A, and Leach K (2015) Biased agonism and biased allosteric modulation at the CB1 cannabinoid receptor. *Mol Pharmacol* **88**: 368–379.

Kloster E, Saft C, Epplen JT, and Arning L (2013) CNR1 variation is associated with the age at onset in Huntington disease. *Eur J Med Genet* **56**: 416–419.

Koppel BS, Brust JC, Fife T, Bronstein J, Youssof S, Gronseth G, and Gloss D (2014) Systematic review: efficacy and safety of medical marijuana in selected neurologic disorders: report of the Guideline Development Subcommittee of the American Academy of Neurology. *Neurology* **82**: 1556–1563.

Kondo S, Kondo H, Nakane S, Kodaka T, Tokumura A, Waku K, Sugiura T (1998) 2-Arachidonoylglycerol, an endogenous cannabinoid receptor agonist: identification as one of the major species of monoacylglycerols in various rat tissues, and evidence for its generation through CA2+-dependent and -independent mechanisms. *FEBS Lett* **429**: 152–156.

Kumar A, Kumar Singh S, Kumar V, Kumar D, Agarwal S, and Rana MK (2015) Huntington's disease: an update of therapeutic strategies. *Gene* **556**: 91–97.

Laprairie RB, Kelly ME, and Denovan-Wright EM (2013) Cannabinoids increase type 1 cannabinoid receptor expression in a cell culture model of striatal neurons: Implications for Huntington's disease. *Neuropharmacology* **72**: 47–57.

Laprairie RB, Bagher AM, Kelly ME, Dupré DJ, and Denovan-Wright EM (2014) Type 1 cannabinoid receptor ligands display functional selectivity in a cell culture

model of striatal medium spiny projection neurons. *J Biol Chem* **289**: 24845–24862.

Laprairie RB, Bagher AM, Kelly ME, and Denovan-Wright EM (2015) Cannabidiol is a negative allosteric modulator of the type 1 cannabinoid receptor. *Br J Pharmcol* **172**: 4790-4805.

Lauckner JE, Hille B, and Mackie K (2005) The cannabinoid agonist WIN55,212-2 increases intracellular calcium via CB1 receptor coupling to Gq/11 G proteins. *Proc Natl Acad Sci U S A* **102**: 19144–19149.

Luttrell LM, Maudsley S, and Bohn LM (2015) Fulfilling the promise of "biased" G protein-coupled receptor agonism. *Mol Pharmacol* **88**: 579–588.

MacCoubrey IC, Moore PL, and Haugland RP (1990) Quantitative fluorescence measurements of cell viability (cytotoxicity) with a multi-well plate scanner. *J Cell Biol* **111**: 303.

McKenzie FR and Milligan G (1991) Cholera toxin impairment of opioid-mediated inhibition of adenylate cyclase in neuroblastoma x glioma hybrid cells is due to a toxin-induced decrease in opioid receptor levels. *Biochem J* **275**: 175–181.

McCaw EA, Hu H, Gomez GT, Hebb AL, Kelly ME, and Denovan-Wright EM (2004) Structure, expression and regulation of the cannabinoid receptor gene (CB1) in Huntington's disease transgenic mice. *Eur J Biochem* **271**: 4909–4920.

McPartland JM, Duncan M, Di Marzo V, and Pertwee RG (2015) Are cannabidiol and Δ(9) -tetrahydrocannabivarin negative modulators of the endocannabinoid system? A systematic review. *Br J Pharmacol* **172**: 737–763.

Mievis S, Blum D, and Ledent C (2011) Worsening of Huntington disease phenotype in CB1 receptor knockout mice. *Neurobiol Dis* **42**: 524–529.

Milligan G, Unson CG, and Wakelam MJ (1989) Cholera toxin treatment produces down-regulation of the alpha-subunit of the stimulatory guanine-nucleotide-binding protein (Gs). *Biochem J* **262**: 643–649.

Meisel K and Friedman JH (2012) Medical marijuana in Huntington's disease: report of two cases. *Med Health RI* **95**: 178–179.

Müller-Vahl KR, Kolbe H, Schneider U, and Emrich HM (1999) Cannabis in movement disorders. *Forsch Komplementarmed* **3**: 23–27.

Naydenov AV, Sepers MD, Swinney K, Raymond LA, Palmiter RD, and Stella N (2014) Genetic rescue of CB1 receptors on medium spiny neurons prevents loss of excitatory striatal synapses but not motor impairment in HD mice. *Neurobiol Dis* **71**: 140–150.

Pamplona FA, Ferreira J, Menezes de Lima O Jr, Duarte FS, Bento AF, Forner S, Villarinho JG, Bellocchio L, Wotjak CT, Lerner R, Monory K, Lutz B, Canetti C, Matias I, Calixto JB, Marsicano G, Guimarães MZ, and Takahashi RN (2012) Anti-inflammatory lipoxin A4 is an endogenous allosteric enhancer of CB1 cannabinoid receptor. *Proc Natl Acad Sci U S A* **109**: 21134–21139.

Paoletti P, Vila I, Rifé M, Lizcano JM, Alberch J, and Ginés S (2008) Dopaminergic and Glutamatergic Signaling Crosstalk in Huntington's Disease Neurodegeneration: The Role of p25/Cyclin-Dependent Kinase 5. *Neurobiol Dis* **28**: 10090–10101.

Pertwee RG (2008) Ligands that target cannabinoid receptors in the brain: from THC to anandamide and beyond. *Addict Biol* **13**: 147–159.

Pazos MR, Mohammed N, Lafuente H, Santos M, Martínez-Pinilla E, Moreno E, Valdizan E, Romero J, Pazos A, Franco R, Hillard CJ, Alvarez FJ, and Martínez-Orgado J (2013) Mechanisms of cannabidiol neuroprotection in hypoxic-ischemic newborn pigs: role of 5HT(1A) and CB2 receptors. *Neuropharmacology* **71**: 282–291.

Russo EB, Burnett A, Hall B, and Parker KK (2005) Agonistic properties of cannabidiol at 5-HT1a receptors. *Neurochem Res* **30**: 1037–1043.

Ryberg E, Larsson N, Sjögren S, Hjorth S, Hermansson NO, Leonova J, Elebring T, Nilsson K, Drmota T, Greasley PJ (2007) The orphan receptor GPR55 is a novel cannabinoid receptor. *Br J Pharmacol* **152**: 1092–1101.

Sadri-Vakili G, Menon AS, Farrell LA, Keller-McGandy CE, Cantuti-Castelvetri I, Standaert DG, Augood SJ, Yohrling GJ, Cha JH (2006) Huntingtin inclusions do not down-regulate specific genes in the R6/2 Huntington's disease mouse. *Eur J Neurosci* **23**: 3171–3175.

Sagredo O, Ramos JA, Decio A, Mechoulam R, and Fernández-Ruiz J (2007) Cannabidiol reduced the striatal atrophy caused 3-nitropropionic acid in vivo by mechanisms independent of the activation of cannabinoid, vanilloid TRPV1 and adenosine A2A receptors. *Eur J Neurosci* **26**: 843–851.

Sagredo O, Pazos MR, Satta V, Ramos JA, Pertwee RG, and Fernández-Ruiz J (2011) Neuroprotective effects of phytocannabinoid-based medicines in experimental models of Huntington's disease. *J Neurosci Res* 89: 1509–1518.

Sim-Selley LJ and Martin BR (2002) Effect of chronic administration of R-(+)-[2,3-Dihydro-5-methyl-3-[(morpholinyl)methyl]pyrrolo[1,2,3-de]-1,4-benzoxazinyl]-

(1-naphthalenyl)methanone mesylate (WIN55,212-2) or delta(9)-tetrahydrocannabinol on cannabinoid receptor adaptation in mice. *J Pharmacol Exp Ther* **303**: 36–44.

Trettel F, Rigamonti D, Hilditch-Maguire P, Wheeler VC, Sharp AH, Persichetti F, Cattaneo E, MacDonald ME (2000) Dominant phenotypes produced by the HD mutation in STHdh(Q111) striatal cells. *Hum Mol Genet* **9**: 2799–2809.

Valdeolivas S, Satta V, Pertwee RG, Fernández-Ruiz J, and Sagredo O (2012) Sativex-like combination of phytocannabinoids is neuroprotective in malonate-lesioned rats, an inflammatory model of Huntington's disease: role of CB1 and CB2 receptors. *ACS Chem Neurosci* **3**: 400–406.

Van Laere K, Casteels C, Dhollander I, Goffin K, Grachev I, Bormans G, Vandenberghe W (2010) Widespread decrease of type 1 cannabinoid receptor availability in Huntington disease in vivo. *J Nucl Med* **51**: 1413–1417.

Wootten D, Christopoulos A, and Sexton PM (2013). Emerging paradigms in GPCR allostery: implications for drug discovery. *Nat Rev Drug Discov* **12**: 630–644.

Molecular Pharmacology Fast Forward. Published on December 23, 2015 as DOI: 10.1124/mol.115.101980
This article has not been copyedited and formatted. The final version may differ from this version.

Footnotes

This work was supported by a partnership grant from the Canadian Institutes of Health Research, Nova Scotia Health Research Foundation, and the Huntington Society of Canada [ROP-97185] to EMD-W, and a Canadian Institutes of Health Research operating grant [MOP-97768] to MEMK. RBL is supported by studentships from the Canadian Institutes of Health Research, the Huntington Society of Canada, Killam Trusts, and Nova Scotia Health Research Foundation. AMB is supported by scholarships from Dalhousie University and King Abdul Aziz University, Jeddah, Saudi Arabia.

This work has been included in the thesis: Laprairie RB (2016). Biased agonists and allosteric modulators: potential treatments for Huntington disease. *Doctoral thesis in the Department of Pharmacology* Dalhousie University, Halifax NS CAN; and was presented in the following conference abstract: Laprairie RB, Bagher AM, Kelly ME, Dupre DJ, and Denovan-Wright EM (2014) The therapeutic efficacy of cannabinoid receptor type 1 (CB1) ligands in Huntington's disease may depend on their functional selectivity. *Experimental Biology & American Society for Pharmacology and Experimental Therapeutics Annual Meeting*. San Diego CA USA, April 25 – May 1, 2014.

Reprint requests shall be sent to: Eileen M Denovan-Wright, Department of Pharmacology, Dalhousie University, 5850 College St. Halifax NS CAN B3H4R2, E-mail: emdenova@dal.ca, Phone: 1.902.494.1363, Fax: 1.902.494.1388

Departments of Pharmacology and Opthamology and Visual Sciences, Dalhousie University, Halifax NS Canada B3H 4R2

Molecular Pharmacology Fast Forward. Published on December 23, 2015 as DOI: 10.1124/mol.115.101980
This article has not been copyedited and formatted. The final version may differ from this version.

Figure Legends

Figure 1. Functional selectivity of cannabinoids in wild-type and mHtt-expressing cells. ST*Hdh*$^{Q7/Q7}$ **(A-E**) and ST*Hdh*$^{Q111/Q111}$ **(F-J)** cells were treated with 10 – 10,000 nM WIN, CP, 2-AG, AEA, THC, CBD, or THC+CBD (1:1) and ERK1/2 phosphorylation (10 min) **(A,F)**, β-arrestin1 recruitment (30 min) **(B,G)**, CREB phosphorylation (30 min) **(C,H)**, PLCβ3 phosphorylation (10 min) **(D,I)**, or Akt phosphorylation (10 min) **(E,J)** were measured and expressed relative to WIN E_{max} in ST*Hdh*$^{Q7/Q7}$ cells. ERK1/2, CREB, PLCβ3, and Akt phosphorylation were measured *via* In-cell western™. β-arrestin1 recruitment was measured *via* BRET[2]. CRCs were fit to the Black-Leff global non-linear regression using the operational model. $N = 4$.

Figure 2. Calculated bias factor of cannabinoids in wild-type and mHtt-expressing cells. Ligand bias (ΔΔlogR) was calculated using eq. 2 as the difference between the ERK ($G\alpha_{i/o}$) response and a second response X: **A)** β-arrestin1, **B)** $G\alpha_s$, **C)** $G\alpha_q$, or **D)** $G\beta\gamma$, Data are displayed as the mean with the minimum and maximum (box) and 95% confidence intervals (error bars). *$P < 0.01$ compared to 0 (*i.e.* no bias), †$P < 0.01$ compared to ST*Hdh*$^{Q7/Q7}$ cells within ligand. $N = 4$.

Figure 3. Changes in functionality and viability in wild-type and mHtt-expressing cells treated with cannabinoids. ST*Hdh*$^{Q7/Q7}$ **(A-D**) and ST*Hdh*$^{Q111/Q111}$ **(E-H)** cells were treated with 10 – 10,000 nM WIN, CP, 2-AG, AEA, THC, CBD, or THC+CBD (1:1) for 30 min and ATP **(A,E)**, change in GABA release compared to vehicle treatment (ΔGABA) **(B,F)**, % cellular esterase activity compared to vehicle treatment **(C,G)**, and %

Molecular Pharmacology Fast Forward. Published on December 23, 2015 as DOI: 10.1124/mol.115.101980
This article has not been copyedited and formatted. The final version may differ from this version.

membrane permeable cells compared to vehicle treatment **(D,H)** were measured. [ATP] was determined using the CellTiter Glo assay (Promega). [GABA] in cell culture media was determined using GABA ELISA assay (Novatein Biosciences). % cellular esterase activity (calcein AM cleavage) and % membrane permeable cells (ethidium homodimer-1 penetration) were determined using the Live/Dead cytotoxicity assay (Invitrogen). CRCs were fit using non-linear regression models. $N = 4$.

Figure 4. Long-term exposure to cannabinoids effected CB_1 localization and levels. ST*Hdh*$^{Q7/Q7}$ and ST*Hdh*$^{Q111/Q111}$ cells were treated with 1.0 µM 2-AG, AEA, WIN, CP, THC, CBD, or THC+CBD (1:1) for 12 h and total CB_1 levels **(A)** and the fraction of CB_1 at the plasma membrane **(B)**. **A)** Total CB_1 levels were determined using In-cell western™ and expressed relative to β-actin levels. $N = 8$. **B)** The fraction of CB_1 at the plasma membrane was determined using On- and In-cell western™. $N = 8$. $^*P < 0.01$ compared to vehicle-treated cells within cell type, $\dagger P < 0.01$ compared to ST*Hdh*$^{Q7/Q7}$ cells within treatment group, as determined using two-way ANOVA followed by Bonferroni's *post-hoc* analysis.

Figure 5. CB_1-independent CREB signalling. A,B) $5HT_{1A}$-dependent CREB signalling. ST*Hdh*$^{Q7/Q7}$ cells were treated with 0.1 – 100,000 nM 8-OH-DPAT, WAY 100635, or CBD ± 1 µM CBD, 100 nM WAY 100635, or 500 nM O-2050 for 30 min and CREB phosphorylation was measured *via* In-cell western™. $N = 4$. **C)** D_2-dependent CREB signalling ST*Hdh*$^{Q7/Q7}$ cells were treated with 0.1 – 100,000 nM CP, quinpirole, or haloperidol ± 10 µM haloperidol, 1 µM quinpirole, or 500 nM O-2050 for 30 min and

Molecular Pharmacology Fast Forward. Published on December 23, 2015 as DOI: 10.1124/mol.115.101980
This article has not been copyedited and formatted. The final version may differ from this version.

CREB phosphorylation was measured *via* In-cell western™. CRCs were fit using non-linear regression models. $N = 4$. All data are expressed relative to WIN E_{max} in ST*Hdh*$^{Q7/Q7}$ cells.

Table 1. pEC_{50} and E_{max} of cannabinoid ligands at CB_1 in ST*Hdh*$^{Q7/Q7}$ and ST*Hdh*$^{Q111/Q111}$ cells.

		ERK response (Gαi/o)				BRET response (β-arrestin1)				CREB response (Gαs)				PLCβ3 response (Gαq)				Akt response (Gβγ)			
		pEC_{50}		E_{max} (%)		pEC_{50}		E_{max} (%)		pEC_{50}		E_{max} (%)		pEC_{50}		E_{max} (%)		pEC_{50}		E_{max} (%)	
WIN	ST*Hdh*$^{Q7/Q7}$	6.3	± 0.4	101	± 4.0	6.2	± 0.5	102	± 3.6	6.7	± 0.2	115	± 10	6.5	± 0.8	105	± 5.9	6.2	± 0.8	102	± 6.4
	ST*Hdh*$^{Q111/Q111}$	6.3	± 0.9	51.5	± 4.1*	6.1	± 0.3	102	± 4.3	7.0	± 0.3	105	± 6.1	6.5	± 0.7	102	± 5.3	6.2	± 0.4	102	± 5.6
CP	ST*Hdh*$^{Q7/Q7}$	6.3	± 0.6	88.0	± 4.7†	7.4	± 0.2†	128	± 4.0†	6.6	± 0.5	443	± 3.6†	6.2	± 0.4	71.8	± 2.9†	6.2	± 0.5	68.1	± 2.7†
	ST*Hdh*$^{Q111/Q111}$	6.4	± 0.5	41.4	± 4.7*	6.9	± 0.1†	126	± 5.1†	6.6	± 0.7	432	± 5.1†	6.2	± 0.4	70.8	± 4.1†	6.2	± 0.7	76.0	± 4.2†
2-AG	ST*Hdh*$^{Q7/Q7}$	6.4	± 0.6	75.2	± 3.6†	6.1	± 0.7	101	± 2.7	N.C.		N.C.		6.3	± 0.6	87.4	± 4.8	6.4	± 0.8	111	± 5.7
	ST*Hdh*$^{Q111/Q111}$	6.3	± 0.6	54.5	± 3.6*	6.2	± 0.3	96.7	± 3.9	N.C.		N.C.		6.2	± 0.6	87.4	± 3.6	6.4	± 0.7	102	± 4.5
AEA	ST*Hdh*$^{Q7/Q7}$	6.4	± 0.8	117	± 5.9†	6.1	± 0.4	76.1	± 2.0†	N.C.		N.C.		6.4	± 0.9	101	± 5.1	6.6	± 0.9	115	± 5.2
	ST*Hdh*$^{Q111/Q111}$	6.5	± 1.7	64.5	± 5.9*†	6.1	± 0.7	65.0	± 4.6†	N.C.		N.C.		6.4	± 0.8	90.2	± 4.8	6.5	± 0.4	111	± 2.8
THC	ST*Hdh*$^{Q7/Q7}$	6.0	± 1.0	40.3	± 2.4†	6.4	± 0.5	98.8	± 3.8	N.C.		N.C.		6.5	± 1.4	71.4	± 6.2†	6.5	± 1.0	48.3	± 6.7†
	ST*Hdh*$^{Q111/Q111}$	5.5	± 1.5	33.8	± 4.7*†	6.4	± 0.4	107	± 9.8	N.C.		N.C.		6.4	± 1.5	67.9	± 5.2†	6.5	± 1.5	40.1	± 5.2†
CBD	ST*Hdh*$^{Q7/Q7}$	N.C.		N.C.		N.C.		N.C.		6.2	± 0.6	445	± 13.1†	N.C.		N.C.		N.C.		N.C.	
	ST*Hdh*$^{Q111/Q111}$	N.C.		N.C.		N.C.		N.C.		6.4	± 0.8	348	± 24.1†	N.C.		N.C.		N.C.		N.C.	
THC + CBD	ST*Hdh*$^{Q7/Q7}$	N.C.		N.C.		6.0	± 0.5	90.2	± 3.0	6.2	± 0.9	204	± 4.4†	6.4	± 0.7	55.4	± 3.3†	6.0	± 0.5	30.3	± 3.2†
	ST*Hdh*$^{Q111/Q111}$	5.0	± 1.1†	17.6	± 2.3†	5.9	± 0.5	102	± 3.4	6.2	± 1.1	194	± 2.9†	6.4	± 1.1	51.1	± 2.8†	6.1	± 0.6	33.2	± 2.7†

Determined using non-linear regression analysis (4 parameters) in GraphPad v. 5.0. E_{max} (%) is the maximal agonist effect relative to E_{max} for WIN in ST*Hdh*$^{Q7/Q7}$ cells for each measurement. Data are expressed as mean ± S.E.M. N.C., not converged.

*P < 0.01 compared to ST*Hdh*$^{Q7/Q7}$ within ligand and measurement. †P < 0.01 compared to WIN within cell type and measurement, as determined using two-way ANOVA followed by Bonferroni's *post-hoc* test (n = 4).

Molecular Pharmacology Fast Forward. Published on December 23, 2015 as DOI: 10.1124/mol.115.101980
This article has not been copyedited and formatted. The final version may differ from this version.

Table 2. Transduction coefficients and relative activity of cannabinoid ligands at CB_1 in ST*Hdh*$^{Q7/Q7}$ and ST*Hdh*$^{Q111/Q111}$ cells.

		ERK response (Gαi/o)				BRET response (β-arrestin1)			
		logR (τ/K_A)		ΔlogR (τ/K_A)[a]		logR (τ/K_A)		ΔlogR (τ/K_A)[a]	
WIN	ST*Hdh*$^{Q7/Q7}$	6.35	(6.33-6.37)	Reference ligand		6.41	(6.36-6.46)	Reference ligand	
	ST*Hdh*$^{Q111/Q111}$	6.33	(6.28-6.38)	Reference ligand		6.41	(6.38-6.44)	Reference ligand	
CP	ST*Hdh*$^{Q7/Q7}$	6.30	(6.26-6.34)	-0.04	(-0.09-0.01)	6.46	(6.41-6.52)	0.05	(-0.03-0.13)
	ST*Hdh*$^{Q111/Q111}$	6.22	(6.17-6.27)	-0.11	(-0.22-0.02)	6.47	(6.42-6.49)	0.06	(-0.01-0.11)
2-AG	ST*Hdh*$^{Q7/Q7}$	6.28	(6.20-6.36)	-0.07	(-0.14-0.00)	6.15	(5.91-6.37)	-0.23	(-0.24- -0.22)*†
	ST*Hdh*$^{Q111/Q111}$	6.28	(6.21-6.35)	-0.05	(-0.11-0.01)	6.27	(6.36-6.38)	-0.13	(-0.23- -0.03)*
AEA	ST*Hdh*$^{Q7/Q7}$	6.35	(6.34-6.36)	0.00	(-0.01-0.01)	6.09	(5.82-6.37)	-0.31	(-0.33- -0.29)*†
	ST*Hdh*$^{Q111/Q111}$	6.42	(6.36-6.48)	0.09	(-0.02-0.20)	6.22	(6.07-6.37)	-0.18	(-0.26- -0.10)*†
THC	ST*Hdh*$^{Q7/Q7}$	4.48	(4.43-4.54)*	-1.83	(-2.97- -0.69)*	6.41	(6.40-6.42)†	0.00	(-0.01-0.01)†
	ST*Hdh*$^{Q111/Q111}$	3.26	(3.22-3.30)*^	-3.01	(-4.43- -1.59)*	4.98	(4.94-5.02)*^†	-1.43	(-1.47- -1.39)*^†
CBD	ST*Hdh*$^{Q7/Q7}$		N.C.		N.C.		N.C.		N.C.
	ST*Hdh*$^{Q111/Q111}$		N.C.		N.C.		N.C.		N.C.
THC + CBD	ST*Hdh*$^{Q7/Q7}$	2.06	(1.91-2.21)*	-4.29	(-5.95- -2.63)*	0.83	(-1.91-1.95)*†	-5.58	(-5.60- -5.56)*
	ST*Hdh*$^{Q111/Q111}$	0.35	(-2.01-3.69)*^	-1.40	(-2.77- -0.33)*	4.83	(4.77-4.89)*^†	-1.58	(-1.64- -1.52)*^†

Determined using the operational model global non-linear regression analysis (Eq. 1, 2) in GraphPad v. 5.0. Data are expressed as mean with 95% CI. N.C., not converged. [a]ΔlogR (τ/K_A) calculated as logR (τ/K_A) test ligand - logR (τ/K_A) reference ligand within cell type, where **WIN** is the reference ligand and ΔlogR (τ/K_A) 'WIN' = 0.

*$P < 0.05$ compared to WIN within cell type and measurement, ^$P < 0.05$ compared to ST*Hdh*$^{Q7/Q7}$ within ligand and measurement, †$P < 0.05$ compared to ERK (Gαi/o) within cell type, as determined using non-overlapping CIs ($n = 4$).

Molecular Pharmacology Fast Forward. Published on December 23, 2015 as DOI: 10.1124/mol.115.101980
This article has not been copyedited and formatted. The final version may differ from this version.

Table 2 Continued. Transduction coefficients and relative activity of cannabinoid ligands at CB_1 in ST*Hdh*$^{Q7/Q7}$ and ST*Hdh*$^{Q111/Q111}$ cells.

		CREB response (Gαs)				PLCβ3 response (Gαq)			
		logR (τ/K_A)		ΔlogR (τ/K_A)[a]		logR (τ/K_A)		ΔlogR (τ/K_A)[a]	
WIN	ST*Hdh*$^{Q7/Q7}$	3.43	(3.32-3.54)†	Reference ligand		6.54	(6.32-6.72)	Reference ligand	
	ST*Hdh*$^{Q111/Q111}$	2.22	(2.20-2.24)^†	Reference ligand		6.51	(6.34-6.66)	Reference ligand	
CP	ST*Hdh*$^{Q7/Q7}$	6.47	(6.46-6.48)*	3.01	(2.91-3.11)*†	5.77	(5. 67-5.87)*†	-0.77	(-0.92- -0.62)*†
	ST*Hdh*$^{Q111/Q111}$	5.07	(5.06-5.08)*	2.85	(2.55-3.04)*†	6.32	(4.35-8.29)^	-0.21	(-0.48-0.06)^
2-AG	ST*Hdh*$^{Q7/Q7}$	N.C.		N.C.		6.01	(4.66-7.36)	-0.53	(-0.88- -0.18)*†
	ST*Hdh*$^{Q111/Q111}$	N.C.		N.C.		5.76	(4.99-6.53)	-0.71	(-1.46-0.04)
AEA	ST*Hdh*$^{Q7/Q7}$	N.C.		N.C.		6.31	(6.08-6.54)	-0.23	(-0.47-0.01)
	ST*Hdh*$^{Q111/Q111}$	N.C.		N.C.		5.41	(4.52-5.94)*^†	-1.13	(-1.99- -0.27)*†
THC	ST*Hdh*$^{Q7/Q7}$	N.C.		N.C.		5.45	(5.23-5.67)*†	-1.09	(-1.31- -0.87)*
	ST*Hdh*$^{Q111/Q111}$	N.C.		N.C.		4.33	(3.80-4.86)*^†	-2.18	(-2.69- -1.67)*^
CBD	ST*Hdh*$^{Q7/Q7}$	3.34	(3.29-3.39)	-0.09	(-0.22-0.04)	N.C.		N.C.	
	ST*Hdh*$^{Q111/Q111}$	2.27	(2.24-2.30)	0.03	(-0.01-0.07)	N.C.		N.C.	
THC + CBD	ST*Hdh*$^{Q7/Q7}$	0.26	(-0.40-1.92)*	-3.19	(-3.21- -3.17)*	0.57	(-1.43-1.91)*	-5.97	(-6.20- -5.74)*
	ST*Hdh*$^{Q111/Q111}$	3.28	(3.27-3.30)*†	1.06	(1.04-1.08)*^†	4.25	(3.55-4.95)*^	-2.27	(-2.95- -1.59)*^

Determined using the operational model global non-linear regression analysis (Eq. 1, 2) in GraphPad v. 5.0. Data are expressed as mean with 95% CI. N.C., not converged. [a]ΔlogR (τ/K_A) calculated as logR (τ/K_A) test ligand - logR (τ/K_A) reference ligand within cell type, where **WIN** is the reference ligand and ΔlogR (τ/K_A) 'WIN' = 0.

*P < 0.05 compared to WIN within cell type and measurement, ^P < 0.05 compared to ST*Hdh*$^{Q7/Q7}$ within ligand and measurement, †P < 0.05 compared to ERK (Gαi/o) within cell type, as determined using non-overlapping CIs (n = 4).

Molecular Pharmacology Fast Forward. Published on December 23, 2015 as DOI: 10.1124/mol.115.101980
This article has not been copyedited and formatted. The final version may differ from this version.

Table 2 Continued. Transduction coefficients and relative activity of cannabinoid ligands at CB_1 in ST*Hdh*$^{Q7/Q7}$ and ST*Hdh*$^{Q111/Q111}$ cells.

		Akt response (Gβγ)			
		logR (τ/K_A)		ΔlogR (τ/K_A)[a]	
WIN	ST*Hdh*$^{Q7/Q7}$	6.18	(5.98-6.40)	Reference ligand	
	ST*Hdh*$^{Q111/Q111}$	6.21	(6.13-6.29)	Reference ligand	
CP	ST*Hdh*$^{Q7/Q7}$	5.94	(5.92-5.96)*†	-0.24	(-0.26- -0.22)*†
	ST*Hdh*$^{Q111/Q111}$	5.84	(5.31-6.37)	-0.37	(-0.91-0.17)
2-AG	ST*Hdh*$^{Q7/Q7}$	6.22	(6.19-6.25)	0.02	(-0.01-0.05)
	ST*Hdh*$^{Q111/Q111}$	6.14	(5.96-6.32)	-0.07	(-0.25-0.11)
AEA	ST*Hdh*$^{Q7/Q7}$	6.32	(6.27-6.37)	0.14	(-0.03-0.25)*
	ST*Hdh*$^{Q111/Q111}$	6.25	(5.73-6.77)	0.04	(-0.47-0.55)
THC	ST*Hdh*$^{Q7/Q7}$	5.35	(5.32-5.38)*†	-0.83	(-0.86- -0.80)*†
	ST*Hdh*$^{Q111/Q111}$	4.00	(3.87-4.13)*^	-2.21	(-2.32- -2.10)*^†
CBD	ST*Hdh*$^{Q7/Q7}$	N.C.		N.C.	
	ST*Hdh*$^{Q111/Q111}$	N.C.		N.C.	
THC + CBD	ST*Hdh*$^{Q7/Q7}$	0.31	(-1.39-2.01)*†	-5.87	(-5.97- -5.77)*
	ST*Hdh*$^{Q111/Q111}$	3.59	(3.50-3.68)*^	-2.62	(-2.72- -2.52)*^

Determined using the operational model global non-linear regression analysis (Eq. 1, 2) in GraphPad v. 5.0. Data are expressed as mean with 95% CI. N.C., not converged. [a]ΔlogR (τ/K_A) calculated as logR (τ/K_A) test ligand - logR (τ/K_A) reference ligand within cell type, where **WIN** is the reference ligand and ΔlogR (τ/K_A) 'WIN' = 0.

*$P < 0.05$ compared to WIN within cell type and measurement, ^$P < 0.05$ compared to ST*Hdh*$^{Q7/Q7}$ within ligand and measurement, †$P < 0.05$ compared to ERK (Gαi/o) within cell type, as determined using non-overlapping CIs ($n = 4$).

Figure 1

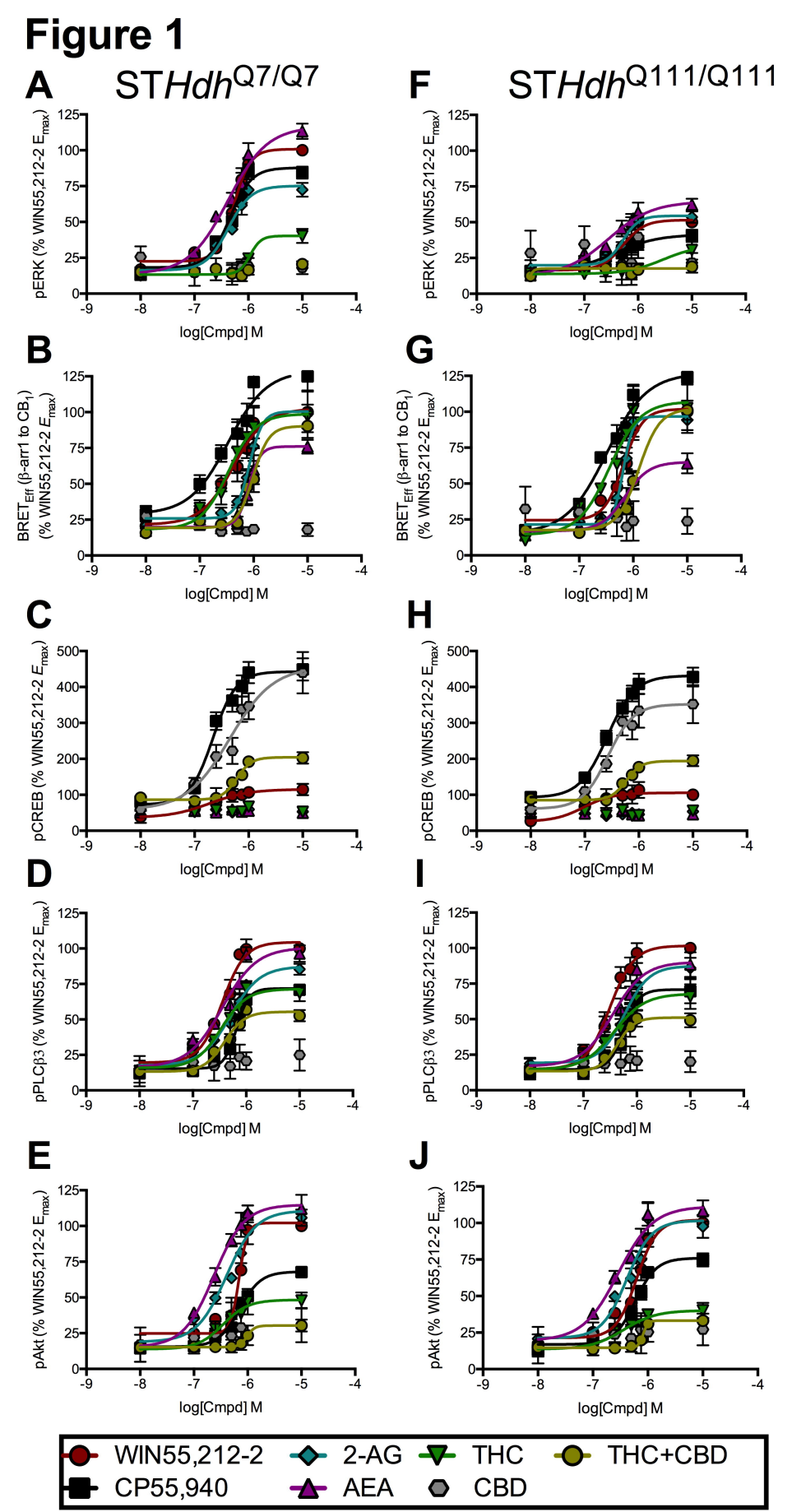
A
STHdhQ7/Q7
F
STHdhQ111/Q111
pERK (% WIN55,212-2 Emax)
BRETEff (β-arr1 to CB1) (% WIN55,212-2 Emax)
pCREB (% WIN55,212-2 Emax)
pPLCβ3 (% WIN55,212-2 Emax)
pAkt (% WIN55,212-2 Emax)
log[Cmpd] M
B
G
C
H
D
I
E
J
WIN55,212-2
CP55,940
2-AG
AEA
THC
CBD
THC+CBD

Figure 2

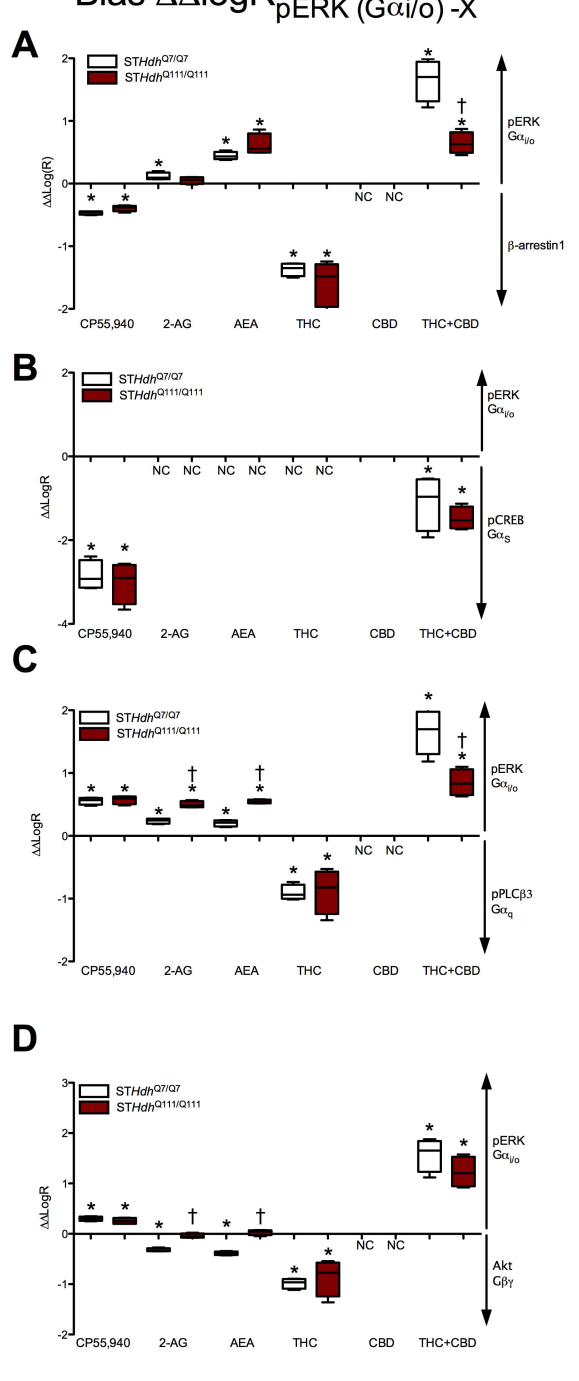
Bias ΔΔlogR pERK (Gαi/o) -X
A
STHdhQ7/Q7
STHdhQ111/Q111
ΔΔLog(R)
pERK Gαi/o
β-arrestin1
NC NC
CP55,940
2-AG
AEA
THC
CBD
THC+CBD
B
ΔΔLogR
pERK Gαi/o
pCREB GαS
C
pERK Gαi/o
pPLCβ3 Gαq
D
pERK Gαi/o
Akt Gβγ

Figure 3

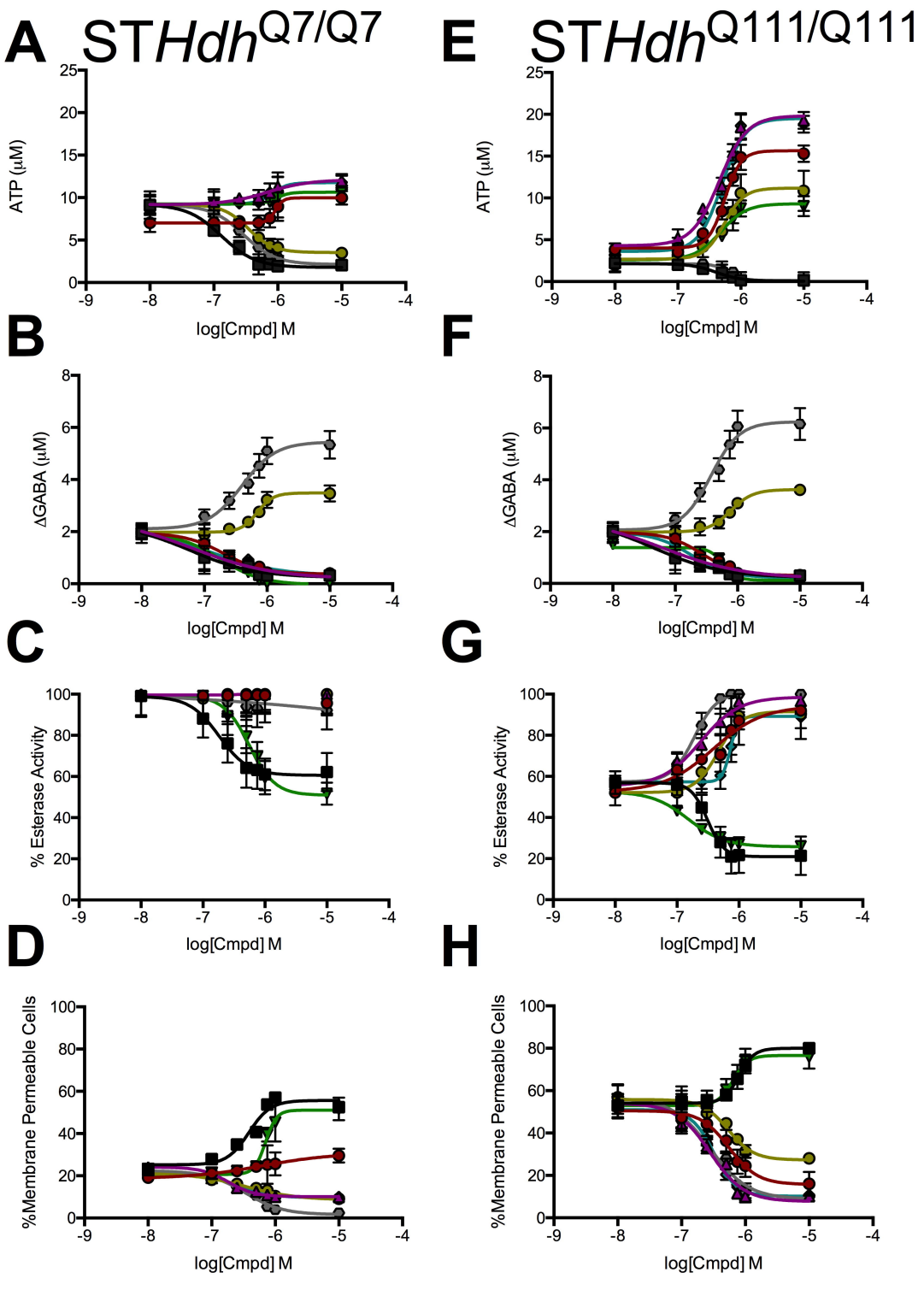
A STHdhQ7/Q7
E STHdhQ111/Q111
ATP (μM)
ΔGABA (μM)
% Esterase Activity
%Membrane Permeable Cells
log[Cmpd] M
B
C
D
F
G
H
WIN55,212-2
CP55,940
2-AG
AEA
THC
CBD
THC+CBD

Figure 4

A

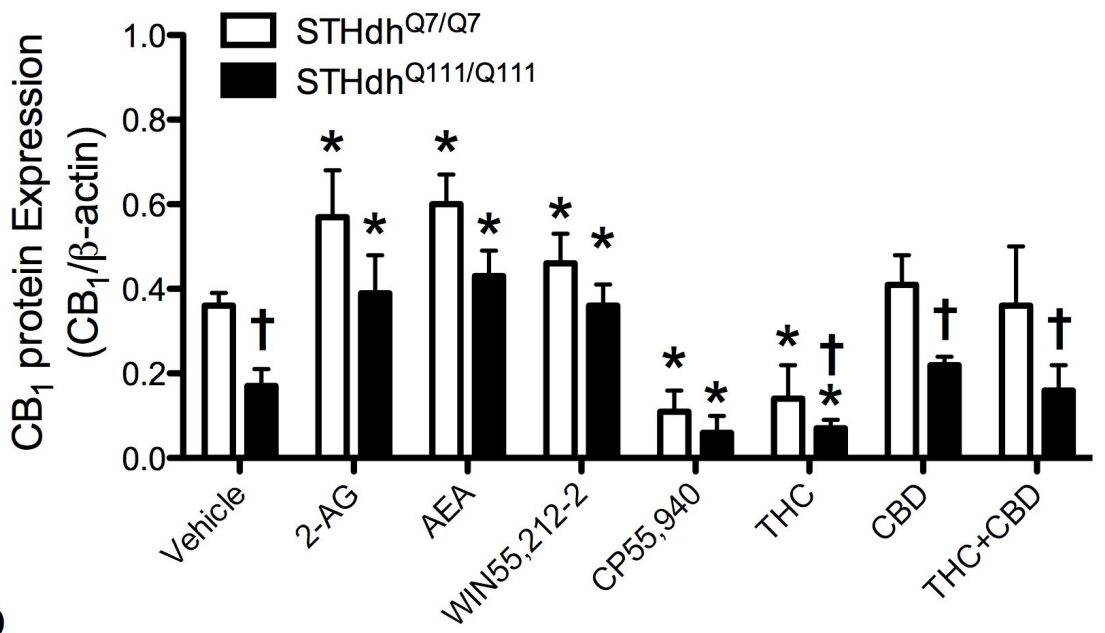
STHdh^Q7/Q7
STHdh^Q111/Q111
CB1 protein Expression (CB1/β-actin)
1.0
0.8
0.6
0.4
0.2
0.0
Vehicle
2-AG
AEA
WIN55,212-2
CP55,940
THC
CBD
THC+CBD

B

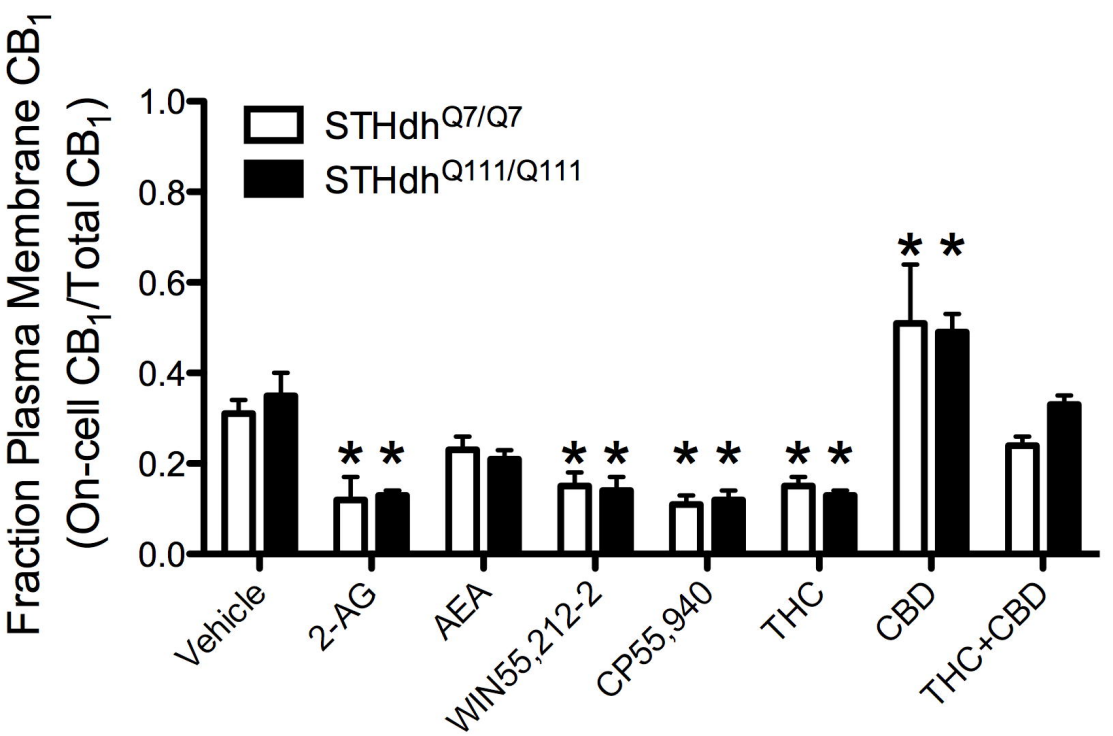
STHdh^Q7/Q7
STHdh^Q111/Q111
Fraction Plasma Membrane CB1 (On-cell CB1/Total CB1)
1.0
0.8
0.6
0.4
0.2
0.0
Vehicle
2-AG
AEA
WIN55,212-2
CP55,940
THC
CBD
THC+CBD

Figure 5

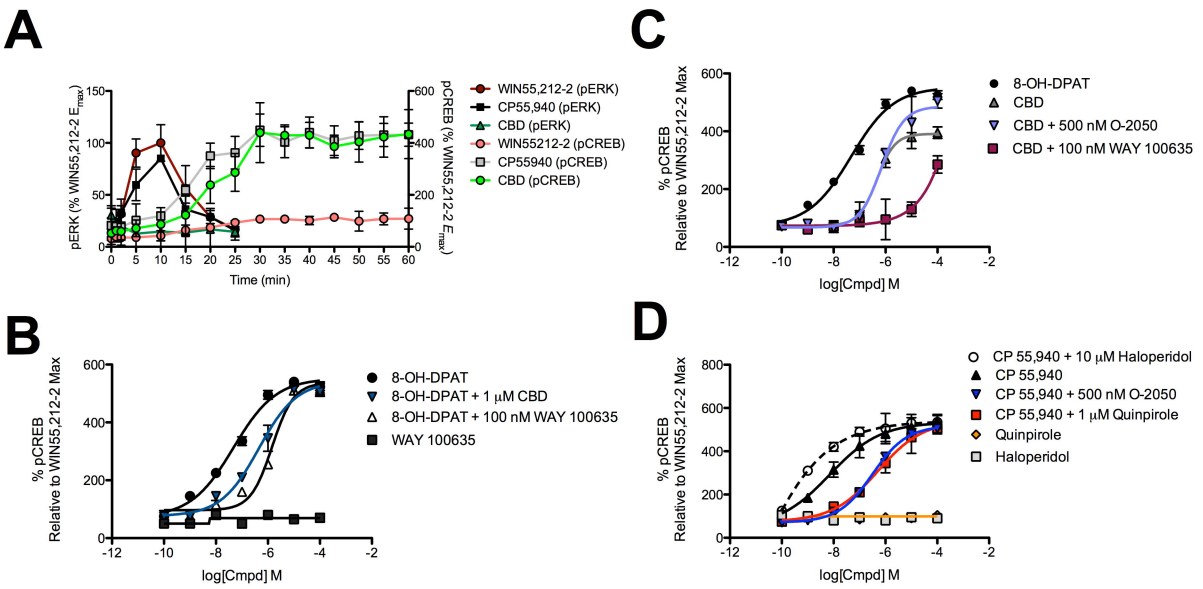
A
pERK (% WIN55,212-2 Emax)
pCREB (% WIN55,212-2 Emax)
Time (min)
WIN55,212-2 (pERK)
CP55,940 (pERK)
CBD (pERK)
WIN55212-2 (pCREB)
CP55940 (pCREB)
CBD (pCREB)
B
% pCREB Relative to WIN55,212-2 Max
log[Cmpd] M
8-OH-DPAT
8-OH-DPAT + 1 μM CBD
8-OH-DPAT + 100 nM WAY 100635
WAY 100635
C
% pCREB Relative to WIN55,212-2 Max
log[Cmpd] M
8-OH-DPAT
CBD
CBD + 500 nM O-2050
CBD + 100 nM WAY 100635
D
% pCREB Relative to WIN55,212-2 Max
log[Cmpd] M
CP 55,940 + 10 μM Haloperidol
CP 55,940
CP 55,940 + 500 nM O-2050
CP 55,940 + 1 μM Quinpirole
Quinpirole
Haloperidol